Electronic Supplementary Information (ESI)

Direct synthesis of triphenylamine-based ordered mesoporous polymers for metal-free photocatalytic aerobic oxidations

Yin Zhu,‡[a] Shengyu Li,‡[a] Xiaorong Yang,[b] Shutao Wang,[a] and Yuan Zhang*[a]

[a] State Key Laboratory of Applied Organic Chemistry, College of Chemistry and Chemical Engineering, Lanzhou University, 222 South Tianshui Road, Lanzhou 730000, P. R. China.

[b] Lanzhou Institute of Husbandry and Pharmaceutical Sciences, Chinese Academy of Agricultural Sciences, Lanzhou 730050, P. R. China.

‡ These authors contributed equally to this work.

E-mail: zhangyuan@lzu.edu.cn.

Table of Contents

A. Summary of Figures and Tables

B. General Information

All reagents were purchased from commercial sources and used as received. *N*-arylglycine derivatives[1,2] were prepared according to literature procedures. All experiments were carried out under air atmosphere, unless otherwise indicated. Irradiation of photochemical reactions was carried out using a 5 W or 24 W blue LED bulb. TLC inspections were taken on silica gel GF254 plates and column flash chromatography was conducted with silica gel (200−300 meshes). The liquid ^{1}H and ^{13}C NMR spectra were recorded on a Bruker Avance 400 MHz spectrometer. The chemical shifts δ are given in ppm relative to tetramethylsilane and the coupling constants J are given in Hz. The spectra were recorded with $CDCl_3$, acetone-d_6, or DMSO-d_6 as solvent at room temperature. Small-angle X-ray diffraction (XRD) patterns were conducted on a PANalytical X'Pert PRO diffractometer with Cu Kα radiation (40 kV, 40 mA). Transmission electron microscopy (TEM) morphologies were observed with a JEOL JEM-1200EX instrument operating at 200 kV. N_2 adsorption and desorption isotherms were measured at 77 K on an ASAP 2020 analyzer. Based on the adsorption branches, the specific surface area (S_{BET}), the average pore diameter (D_P), and the pore volume (V_P) were calculated by using the multiple-point Brunauer-Emmett-Teller (BET) and the Barrett-Joyner-Halenda (BJH) models. The nitrogen content was determined by elemental analysis using an Elementar Analysensysteme GmbH vario EL cube V1.2.1 elemental analyzer. FT-IR spectra were recorded on a Nicolet FT-170SX spectrometer. Samples were prepared by dispersing in anhydrous KBr. Solid-state NMR spectra were obtained on a WB 400 MHz Bruker Avance II spectrometer. The ^{13}C CP/MAS NMR spectra were recorded with the contact time of 2 ms (ramp 100) and the recycle delay of 2 s with a 4-mm double-resonance probe. The diffuse reflectance spectra of the solids were collected at room temperature with a UV-Vis-NIR diffuse reflectance spectrometer (Agilent Technologies, Cary 5000) at a photometric range of 250–800 nm. Ultraviolet photoelectron spectroscopy (UPS) measurements was obtained by using a KRATOS Axis ultra-DLD X-ray photoelectron spectrometer with an unfiltered HeI (21.22 eV) gas discharge lamp and a total instrumental energy resolution of 100 meV. The thermogravimetric analysis (TGA) was performed on a STA 449C Jupiter instrument, with the temperature from ambient to 800 °C under nitrogen atmosphere (heating rate of 10 °C/min).

C. Synthesis of Functional Monomer

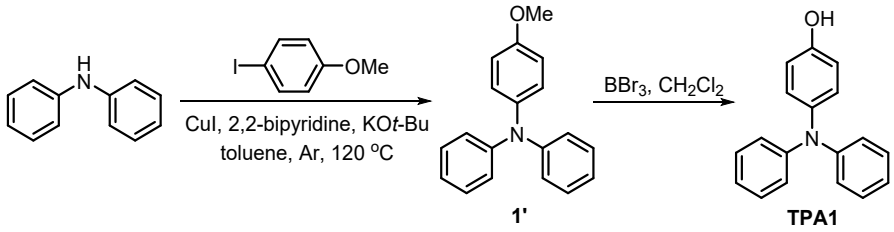

Scheme S1. Synthesis of **TPA1**.

Synthesis of 4-methoxy-*N*, *N*-diphenylaniline (1′).[3] A mixture of 4-iodoanisole (5.14 g, 22.0 mmol), 2,2'-bipyridine (0.13 g, 0.8 mmol), CuI (0.15 g, 0.8 mmol), potassium *tert*-butoxide (3.36 g, 30.0 mol), and diphenylamine (3.38 g, 20.0 mmol) were dissolved in 40 mL of toluene under Ar. The solution was heated to 120 °C for 24 h. After cooling to room temperature, the salt of the mixture was filtrated with celite. The result solution was concentrated to remove solvent under vacuo, and the crude product was purified by the flash chromatography (silica gel, petroleum ether) to obtain a white solid (3.57g, 65%). ^{1}H NMR (400 MHz, $CDCl_3$) δ 7.15–7.10 (m, 4H), 7.01–6.98 (m, 2H), 6.96 (d, J = 7.3 Hz, 4H), 6.86 (t, J = 7.3 Hz, 2H), 6.76 (d, J = 8.9 Hz, 2H), 3.72 (s, 3H); ^{13}C NMR (100 MHz, $CDCl_3$) δ 156.1, 148.2, 140.8, 129.0, 127.3, 122.9, 121.8, 114.7, 55.5.

Synthesis of 4-(diphenylamino)phenol (TPA1).[3] Into a dried round bottom flask was weighed compound **1′** (4.0 g, 14.8 mmol) in 10 mL of CH_2Cl_2. The solution was cooled on an ice bath, and a solution of boron tribromide (2.2 mL, 22.5 mmol) in 20 mL CH_2Cl_2 was added dropwise under Ar. While stirring, the mixture was heated up to room temperature for 6 h. After reaction was completed, the mixture was hydrolyzed with a small amount of 10% aqueous NaOH and acidified with 2M HCl. The result solution was extracted with ethyl acetate, washed with water, dried (Na_2SO_4) and concentrated. The product was purified by the flash chromatography (silica gel, petroleum ether/ EtOAc = 8/1) to obtain the product **TPA1** (2.87g, 74%) as an off-white solid. ^{1}H NMR (400 MHz, $CDCl_3$) δ 7.21 (t, J = 7.9 Hz, 4H), 7.06–7.00 (m, 6H), 6.94 (t, J = 7.3 Hz, 2H), 6.76 (d, J = 8.7 Hz, 2H), 4.60 (s, 1H); ^{13}C NMR (100 MHz, $CDCl_3$) δ 152.0, 148.2, 141.0, 129.1, 127.5, 122.9, 121.9, 116.2.

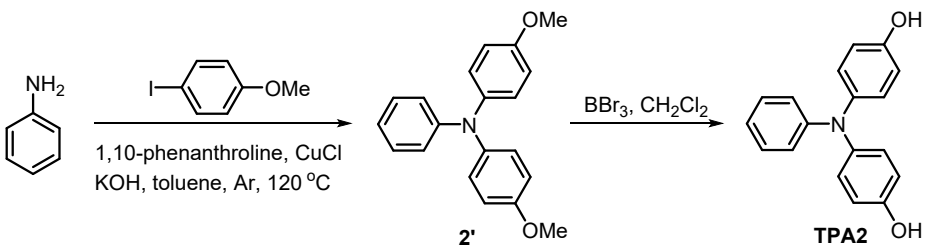

Scheme S2. Synthesis of **TPA2**.

Synthesis of 4-methoxy-*N*-(4-methoxyphenyl)-*N*-phenylbenzenamine (2′).[4] A mixture of 4-iodoanisole (11.23 g, 48.0 mmol), 1,10-phenanthroline (0.72 g, 4.0 mmol), CuCl (0.40 g, 4.0 mmol), KOH (9.0 g, 160.0 mmol), and aniline (1.8 mL, 20.0 mmol) were dissolved in 40 mL of toluene under Ar. The solution was heated to 120 °C for 18 h. After cooling to room temperature, acetic acid was added. The mixture was extracted with ethyl acetate, washed with H_2O and the organic layer was dried over Na_2SO_4. The solution was concentrated to remove solvent under vacuo, and the crude product was purified by the flash chromatography (silica gel, petroleum ether/EtOAc = 16/1). Recrystallization (ethanol) gave the product as a pale yellow crystalline solid (2.92 g, 48%). ^{1}H NMR (400 MHz, $CDCl_3$) δ 7.16 (t, J = 7.8 Hz, 2H), 7.04 (d, J = 8.6 Hz, 4H), 6.93 (d, J = 7.8 Hz, 2H), 6.88–6.79 (m, 5H), 3.78 (s, 6H); ^{13}C NMR (100 MHz, $CDCl_3$) δ 155.7, 148.8, 141.2, 128.9, 126.4, 120.9, 120.6, 114.6, 55.5.

Synthesis of 4, 4'-(phenylazanediyl)diphenol (TPA2).[4] Into a flame dried round bottom flask was weighed of **2′** (3.5 g, 11.5 mmol) in 10 mL of CH_2Cl_2. The solution was cooled on an ice bath, and a solution of boron tribromide (3.3 mL, 34.5 mmol) in 30 mL CH_2Cl_2 was added dropwise under Ar. While stirring, the mixture was heated up to room temperature for 6 h. After reaction was completed, the mixture was hydrolyzed with a small amount of 10% aqueous NaOH and acidified with 2 M HCl. The result solution was extracted with ethyl acetate, washed with water, dried (Na_2SO_4) and concentrated. The product was purified by the flash chromatography (silica gel, petroleum ether/EtOAc = 4/1) to obtain the product **TPA2** (2.9 g, 90 %) as an off-white solid. ^{1}H NMR (400 MHz, DMSO-d_6) δ 9.27 (s, 2H), 7.14–7.08 (m, 2H), 6.92–6.87 (m, 4H), 6.76–6.67 (m, 7H); ^{13}C NMR (100 MHz, DMSO-d_6) δ 153.9, 149.0, 138.7, 128.9, 127.1, 119.1, 118.3, 116.2.

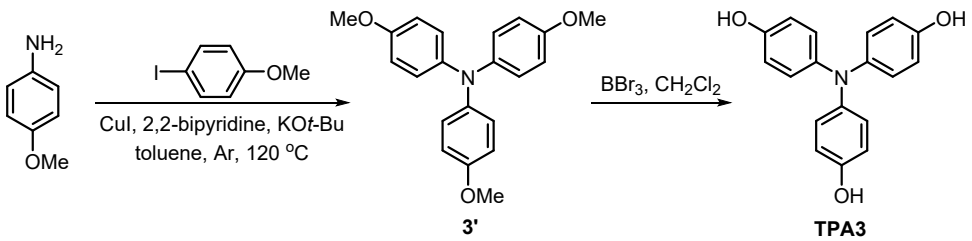

Scheme S3. Synthesis of **TPA3**.

Synthesis of tris(4-methoxyphenyl)amine (3′).[5] A mixture of 4-iodoanisole (9.83 g, 42.0 mmol), 2,2'-bipyridine (0.13 g, 0.8 mmol), CuI (0.15 g, 0.8 mmol), potassium *tert*-butoxide (3.36 g, 60.0 mol), and *p*-anisidine (2.46 g, 20.0 mmol) were dissolved in 40

mL of toluene under Ar. The solution was heated to 120 °C for 18 h. After cooling to room temperature, the salt of the mixture was filtrated with celite. The result solution was concentrated to remove solvent under vacuo, and the crude product was purified by the flash chromatography (silica gel, petroleum ether/EtOAc = 8/1) to obtain a yellow solid (2.48 g, 37%). ^{1}H NMR (400 MHz, $CDCl_3$) δ 6.96 (d, J = 9.0 Hz, 6H), 6.78 (d, J = 9.0 Hz, 6H), 3.77 (s, 9H); ^{13}C NMR (100 MHz, $CDCl_3$) δ 154.9, 142.0, 124.8, 114.5, 55.5.

Synthesis of 4,4',4''-nitrilotriphenol (TPA3).[5] Into a round bottom flask was weighed **3′** (3.72 g, 11.0 mmol) in 10 mL of CH_2Cl_2. The solution was cooled on an ice bath, and a solution of boron tribromide (5.4 mL, 55.5 mmol) in 20 mL CH_2Cl_2 was added dropwise under Ar. While stirring, the mixture was heated up to room temperature for 8 h. After reaction was completed, the mixture was hydrolyzed with a small amount of 10% aqueous NaOH and acidified with 2 M HCl. The result solution was extracted with ethyl acetate, washed with water, dried (Na_2SO_4) and concentrated. The product was purified by the flash chromatography (silica gel, petroleum ether/EtOAc = 2/1) to obtain the product **TPA3** (2.30 g, 72%) as a grey solid. ^{1}H NMR (400 MHz, DMSO-d_6) δ 9.07 (s, 3H), 6.73 (d, J = 8.8 Hz, 6H), 6.64 (d, J = 8.8 Hz, 6H); ^{13}C NMR (100 MHz, DMSO-d_6) δ 152.4, 140.4, 124.5, 115.9.

D. Synthesis of TPA-MPs

Synthesis of triphenylamine-derived resol precursors.[6] The soluble low-molecular-weight triphenylamine-based resol precursor derived from 4-(diphenylamino)phenol **TPA1**, phenol and formaldehyde was prepared by a base-catalyzed polymerization method. Typical synthetic procedure: phenol (0.85 g, 9.0 mmol) was melted at 40–45 ℃ before **TPA1** (0.26g, 1.0 mmol) was added. After that, 20% NaOH (aq; 0.2 g, 1.0 mmol) was added slowly over 5 min with stirring. Then 37 wt% formaldehyde aqueous solution (2.43 g, 30 mmol) was added dropwise, and the reaction mixture was stirred at 72 ℃ for 1.5 h. After the mixture was cooled to room temperature, the mixture pH was adjusted to 7.0 by using 0.6 M HCl aqueous solution. Water was then removed by rotary evaporation below 50 ℃. The final TPA1-derived resol precursor was redissolved in ethanol (6.18 g) before use.

Synthesis of TPA-MP-1.[6] In a typical preparation, triblock copolymer poly (ethyleneoxide)-*b*-poly(propyleneoxide)-*b*-poly(ethylene oxide) (PEO-PPO-PEO, pluronic 127; 1.50 g) was dissolved in ethanol (30.0 g), then the ethanol solution of the above oligomers (7.0 g) was added with stirring for 10 min to form a settled solution. The mixture was transferred to dishes. The ethanol was evaporated at room temperature overnight to produce a membrane and the membrane was heated in an oven at 120 °C for 36 h to thermopolymerize the phenolic resins. The products were calcined at 350 °C under nitrogen for 5 h with the temperature increase rate of 1°C min^{-1} to remove the F127 template. The final ordered mesoporous polymer was denoted as TPA-MP-1.

The synthesis procedure for TPA-MP-2 and TPA-MP-3 were similar to that for TPA-MP-1, starting from 4, 4'-(phenylazanediyl)diphenol **TPA2** (the molar ratios of TPA2/phenol is 1/8) and 4,4',4''-nitrilotriphenol **TPA3** (the molar ratios of TPA3/phenol is 1/7), respectively.[6]

Table S1. Elemental analysis and calculation procedure for the loading amount of TPA-MPs

	C (wt%)	H (wt%)	N (wt%)	Loading amount (mmol/g)
TPA-MP-1	78.44	5.43	0.95	0.68
TPA-MP-2	78.85	5.14	0.86	0.61
TPA-MP-3	77.79	4.82	0.95	0.68

TPA loading amount = 1000 x N content of TPA-MPs/14 mmol/g

E. Characterization of TPA-MPs

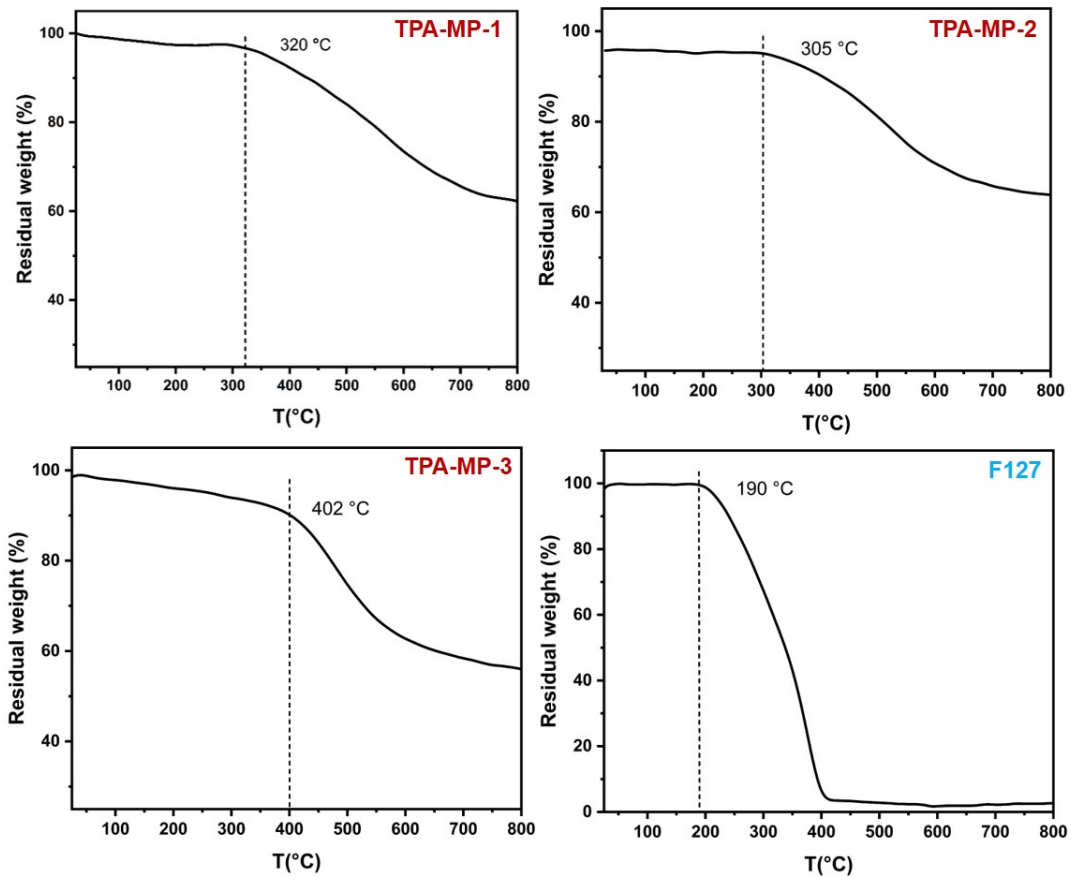

Fig. S1 TGA analysis of TPA-MP-1, TPA-MP-2, TPA-MP-3, and F127.

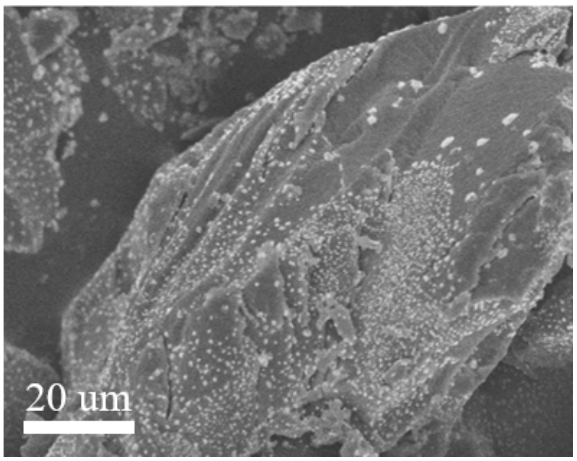

Fig. S2 SEM image of TPA-MP-1.

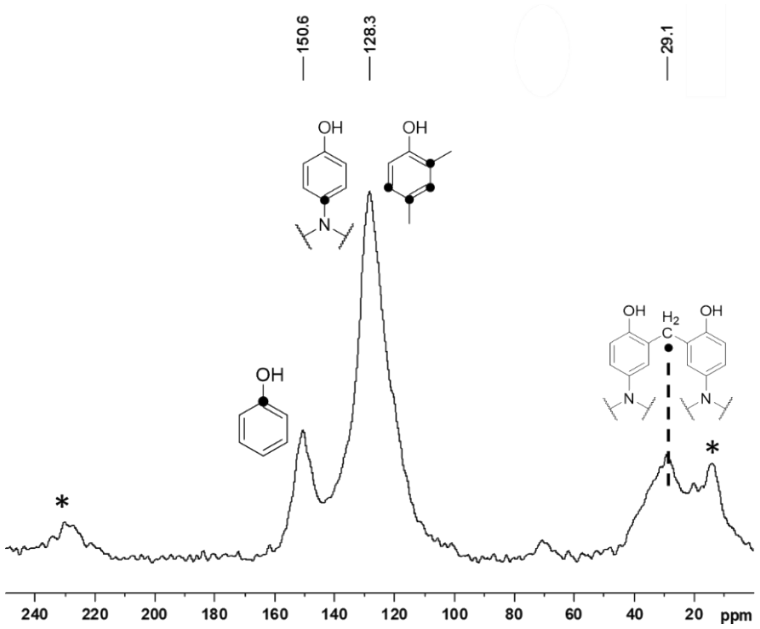

Fig. S3 Solid state ^{13}C CP/MAS NMR spectra of TPA-MP-1.

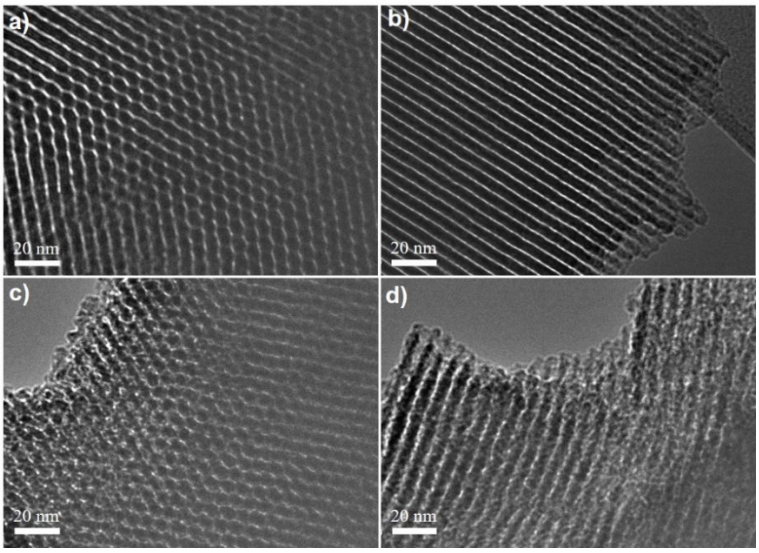

Fig. S4 TEM images of TPA-MP-2 taken along a) [11] direction and b) along [10] direction, and of TPA-MP-3 taken along c) [11] direction and d) along [10] direction.

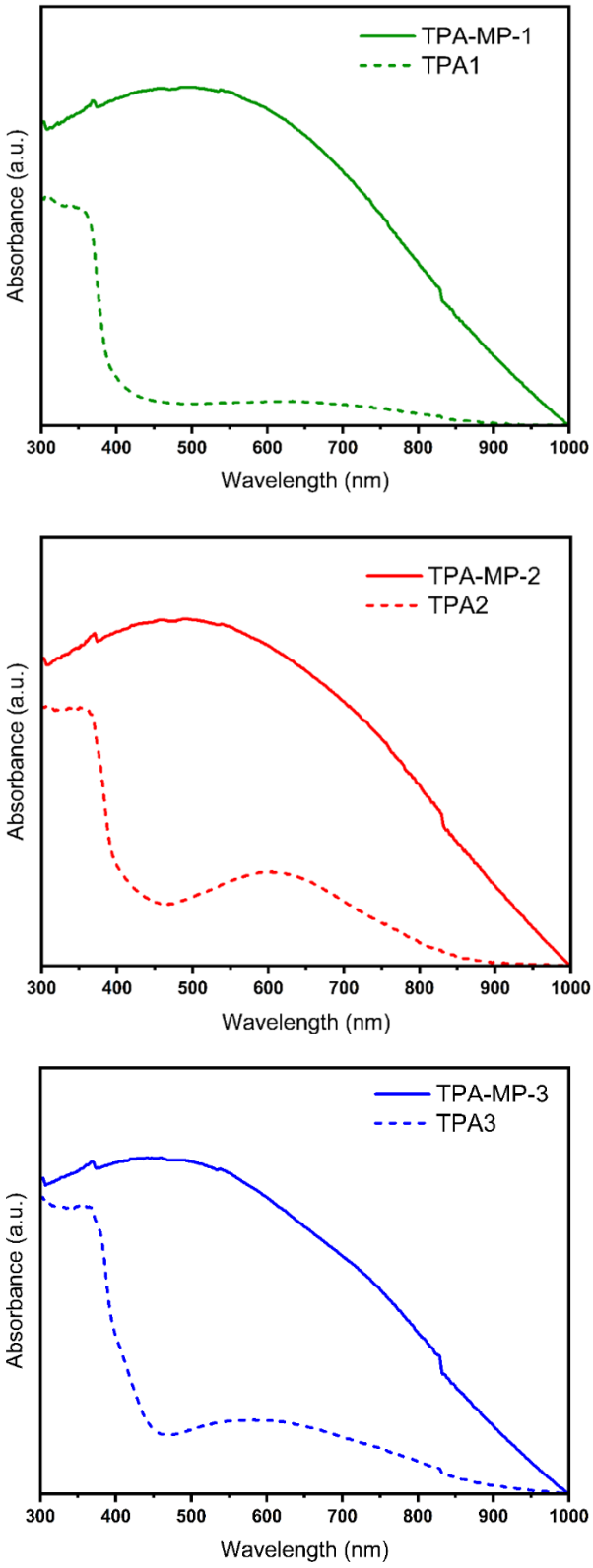

Fig. S5 UV/vis absorption spectra of TPA-MP-1 (green), TPA-MP-2 (red), and TPA-MP-3 (blue).

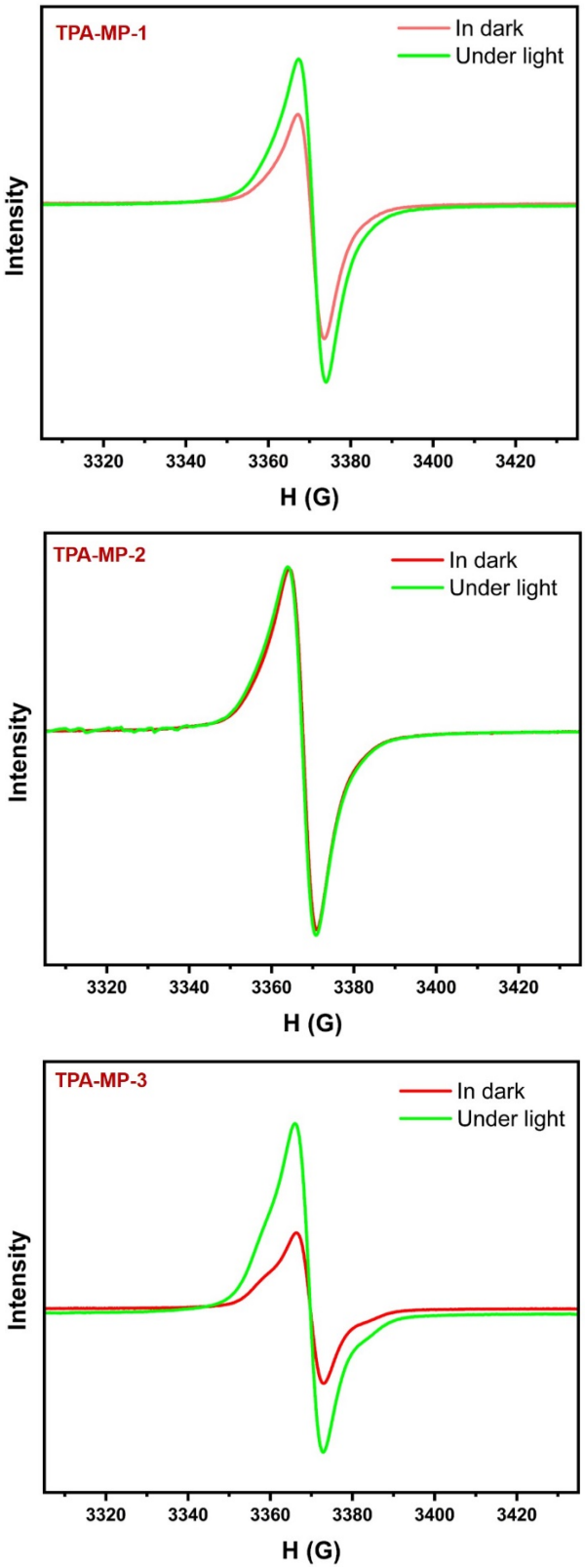

Fig. S6 EPR spectra using TPA-MP-1, TPA-MP-2 and TPA-MP-3 as photocatalyst in dark and under light irradiation, respectively.

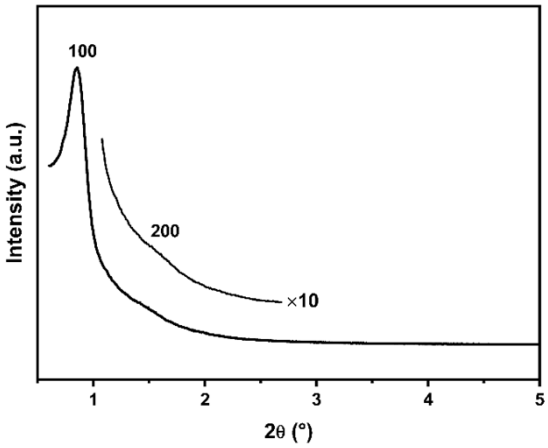

Fig. S7 Small angle XRD pattern of recycled TPA-MP-1 catalyst after 5 times of catalytic reactions.

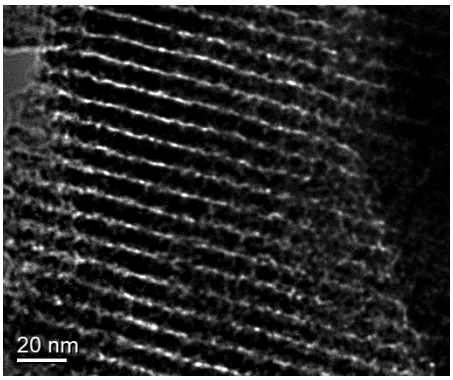

Fig. S8 TEM image of recycled TPA-MP-1 catalyst after 5 times of catalytic reactions.

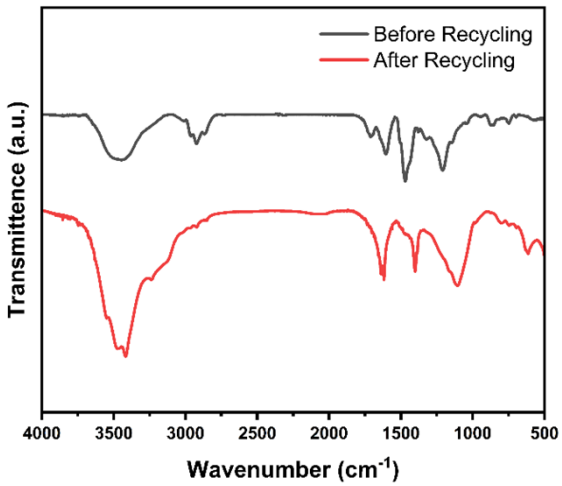

Fig. S9 FT-IR spectra of fresh (black) and recycled TPA-MP-1 catalyst after 5 times of catalytic reactions (red). It was evident that the structure of TPA-MP-1 was not destroyed after catalytic reactions.

F. Computational Studies

Computational methods

All calculations were carried out with the Gaussian 09 D.01programs[7]. Ground state geometry were fully optimized by using density functional theory (DFT) [8] and the B3LYP[9] method with the 6-31G (d,p) basis set all atoms. Frequency calculations have been performed to verify the optimized structures as local minima and to obtain Gibbs free energy at 298 K. The 3D molecular structures were generated using the CYL-view.[10]

Gibbs free energy for the formation of $^1O_2$ and $O_2^{\cdot-}$

$$\text{TPA-MP-1}_{S0} \xrightarrow{h\nu} \text{TPA-MP-1}_{S1} \xrightarrow{ISC} \text{TPA-MP-1}_{T1}$$

0.00 kcal/mol 68.65 kcal/mol

$$\text{ET : TPA-MP-1}_{T1} + {}^3O_2 \longrightarrow \text{TPA-MP-1}_{S0} + {}^1O_2 \quad \Delta G = -28.73 \text{ kcal/mol}$$

$$\text{eT : TPA-MP-1}_{T1} + {}^3O_2 \longrightarrow \text{TPA-MP-1}^{+} + O_2^{\cdot-} \quad \Delta G = 75.98 \text{ kcal/mol}$$

We firstly optimized the singlet and triplet of a cross-section in TPA-MP-1, respectively. The excitation energy required by TPA-MP-1 in photocatalysis was roughly simulated by the energy difference between the singlet and triplet states of TPA-MP-1 to be 68.65 kcal/mol. Next, the free energy of the two photocatalytic processes (energy transfer and electron transfer) of TPA-MP-1 activation was calculated using the triplet state as the excited state by DFT, as shown in Fig. S10. According to the simulation, $^1O_2$ is activated by an exothermic process of -28.73 kcal/mol, while for $O_2^{\cdot-}$, it is an endothermic process of 75.98 kcal/mol. The activation energy of these two processes indicates that $^1O_2$ is more advantageous than the $O_2^{\cdot-}$ in the photoreaction process.

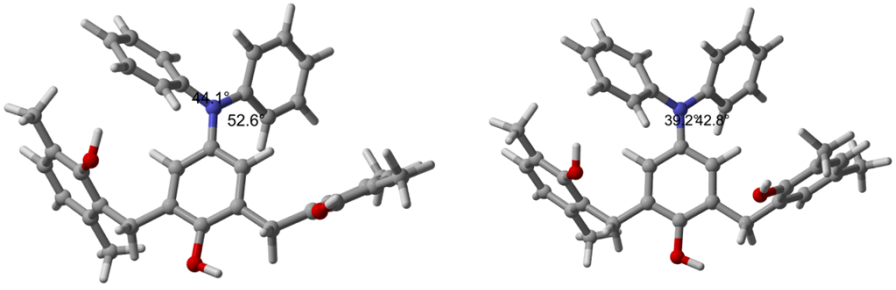

Fig. S10 Optimized structure of the singlet (left) and triplet (right) for TPA-MP-1

(a cross-section).

The LUMO, HOMO distribution of TPA1 and TPA-MP-1

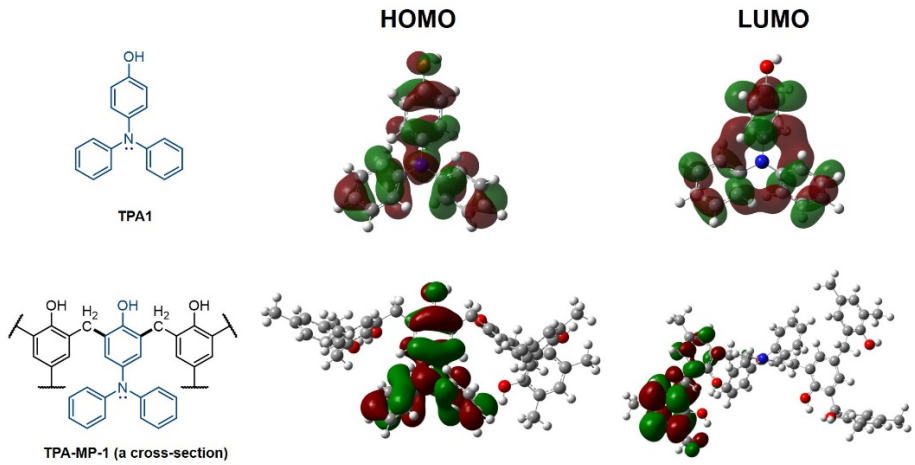

Fig. S11 The LUMO, HOMO distribution of TPA1 and TPA-MP-1 based on the DFT simulation. The HOMO in TPA-MP-1 is not changed much compared with TPA1, mainly concentrated on the triphenylamine segment; while the LUMO in TPA-MP-1 is delocalized over the aromatic rings adjacent to triphenylamine segment. These spatially separated molecular orbitals can favor efficient intramolecular charge transfer, which render TPA-MP-1 an ideal metal-free candidate for photocatalytic applications.

PXRD peak position of TPA1-MP1

As far as we know, the atomic arrangement in FDU-type ordered mesoporous polymer is disordered, and the PXRD diffraction peaks are based on the ordering of mesoporous channels. Therefore, TPA-MP-1 does not have a fixed microscopic chemical order, which makes it impossible for us to obtain its CIF file, so it is difficult to simulate its powder X-ray diffraction results through computational chemistry. However, we tried our best to calculate the approximate PXRD peak position of TPA-MP-1 by using the aperture data obtained by N_2 sorption at 77 K:

$$d = \frac{2\Pi}{q}$$

Where d is the distance between the centers of the two holes (in nm); q is the abscissa value of SAXS data (in nm^{-1}). TPA-MP-1 belongs to the $P6_{mm}$ space group, so its peak position should be roughly at 1.14 nm^{-1}, 1.99 nm^{-1} and 2.28 nm^{-1}.

Solar-to-chemical efficiency

The solar-to-chemical efficiency could be calculated[11] according to the following equation:

$$\text{SCC efficiency (\%)} = \frac{[\Delta G \text{ for } \mathbf{3a} \text{ generation (J mol}^{-1})][\mathbf{3a} \text{ formed (mol)}]}{[\text{total input power (W)}][\text{reaction time (s)}]} \times 100\%$$

Where △G = △H (**3a**) - T△S (**3a**), because the accurate data of △H (**3a**) and △S (**3a**) could not be obtained, therefore, △G can't be calculated exactly.

We accordingly calculated the gibbs free energy for each compound in the following equation and obtain a theoretical gibbs free energy for this reaction (△G = - 3181 kJ/mol).

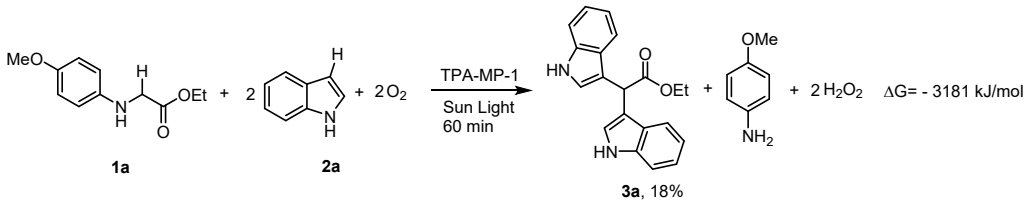

When using TPA-MP-1 as the photocatalyst, the irradiated areas are 10 cm^2 during 60 min of sun illumination. Therefore, the calculated total input energy is 3600 J. During the 60 min photocatalytic reaction, 0.000018 mol **3a** is formed.

SCC efficiency (%) = 3181 x 1000 x 0.000018/3600 = 1.6 %

G. Typical Procedure for Reaction

General procedure for visible-light induced oxidative cross-coupling reaction of glycine derivatives with indoles catalyzed by TPA-MPs.

To a solution of *N*-arylglycine derivative **1** (0.1 mmol, 1 eq), TPA-MPs (1 mol%) and citric acid (0.15 mmol, 1.5 eq) in dry CH_3CN (2.0 mL) was added indole **2** (0.21 mmol, 2.1 eq). The solution was irradiated with a 5 W blue LED bulb under air atmosphere at room temperature. After the reaction was completed, the mixture was diluted with EtOAc, the catalyst was isolated via centrifugation, and thoroughly washed with EtOAc (4 times). The combined organic phase was washed with water and brine, and dried over anhydrous Na_2SO_4. The solvent was removed under reduced pressure, and the residue was separated by silica gel column chromatography (petroleum ether/EtOAc = 4:1) to obtain the product **3**.

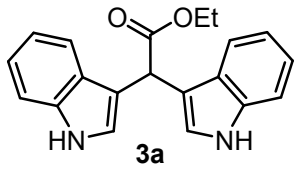

3a

Ethyl 2, 2-di(1H-indol-3-yl)acetate (3a).[12] Pale red powder (27.4 mg, 87%). ^{1}H NMR (400 MHz, $CDCl_3$) δ 7.92 (s, 2H), 7.60 (d, J = 7.9 Hz, 2H), 7.22 (d, J = 8.1 Hz, 2H), 7.17–7.12 (m, 2H), 7.10–7.03 (m, 2H), 6.86 (d, J = 2.1 Hz, 2H), 5.46 (s, 1H), 4.19 (q, J = 7.1 Hz, 2H), 1.23 (t, J = 7.1 Hz, 3H); ^{13}C NMR (100 MHz, $CDCl_3$) δ 173.7, 136.2, 126.5, 123.4, 121.9, 119.4, 119.2, 113.3, 111.3, 6.16, 40.5, 14.2.

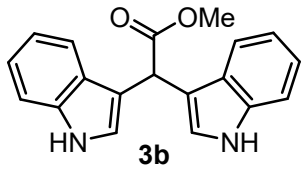

3b

Methyl 2, 2-di(1H-indol-3-yl)acetate (3b).[12] Pale red powder (28.0 mg, 92%). ^{1}H NMR (400 MHz, $CDCl_3$) δ 7.96 (s, 2H), 7.60 (d, J = 7.9 Hz, 2H), 7.24 (t, J = 7.1 Hz, 2H), 7.19–7.12 (m, 2H), 7.08 (t, J = 7.4 Hz, 2H), 6.91 (d, J = 2.3 Hz, 2H), 5.49 (s, 1H), 3.72 (s, 3H); ^{13}C NMR (100 MHz, $CDCl_3$) δ 174.1, 136.2, 126.5, 123.4, 122.0, 119.5, 119.1, 113.2, 111.3, 52.3, 40.3.

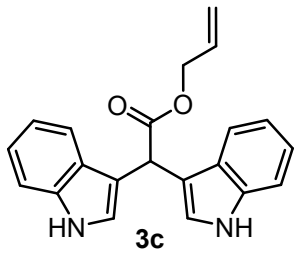

3c

Allyl 2, 2-di(1H-indol-3-yl)acetate (3c).[12] Yellow powder (28.7 mg, 87%). ^{1}H NMR (400 MHz, $CDCl_3$) δ 7.98 (s, 2H), 7.67 (d, J = 7.9 Hz, 2H), 7.32–7.27 (m, 2H), 7.22 (t, J = 7.2 Hz, 2H), 7.17–7.11 (m, 2H), 6.96 (d, J = 2.1 Hz, 2H), 5.94 (m, 1H), 5.58 (s, 1H), 5.34–5.16 (m, 2H), 4.70 (d, J = 5.7 Hz, 2H); ^{13}C NMR (100 MHz, $CDCl_3$) δ 173.3, 136.2, 131.9, 126.5, 123.4, 122.0, 119.5, 119.1, 118.4, 113.2, 111.3, 65.7, 40.4.

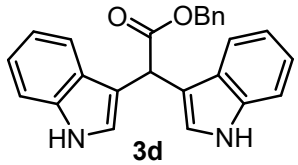

3d

Benzyl 2, 2-di(1H-indol-3-yl)acetate (3d).[12] Pale yellow powder (32.7 mg, 86%). ^{1}H NMR (400 MHz, acetone-d_6) δ 10.17 (s, 2H), 7.61 (d, J = 8.0 Hz, 2H), 7.40 (d, J = 8.2 Hz, 2H), 7.34–7.27 (m, 7H), 7.13–7.07 (m, 2H), 7.00–6.96 (m, 2H), 5.62 (s, 1H), 5.20 (s, 2H); ^{13}C NMR (100 MHz, acetone-d_6) δ 173.6, 137.7, 137.4, 129.2, 128.9, 128.7, 127.7, 124.6, 122.2, 120.0, 119.6, 113.9, 112.2, 66.9, 41.6.

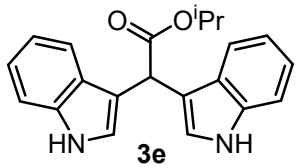

3e

Isopropyl 2, 2-di(1H-indol-3-yl)acetate (3e).[12] Off-white powder (25.3 mg, 76%). ^{1}H NMR (400 MHz, acetone-d_6) δ 10.14 (s, 2H), 7.64 (d, J = 7.9 Hz, 2H), 7.40 (d, J = 8.1 Hz, 2H), 7.25 (d, J = 1.8 Hz, 2H), 7.11–7.07 (m, 2H), 7.01–6.97 (m, 2H), 5.47 (s, 1H), 5.06–4.99 (m, 1H), 1.20 (d, J = 6.3 Hz, 6H); ^{13}C NMR (100 MHz, acetone-d_6) δ 173.2, 137.7, 127.8, 124.5, 122.2, 120.0, 119.5, 114.2, 112.2, 68.5, 41.9, 22.0.

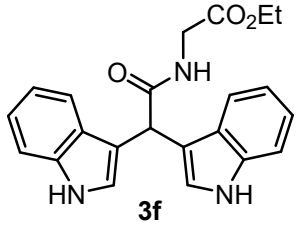

3f

Ethyl (2, 2-di(1H-indol-3-yl)acetyl)glycinate (3f).[12] Pale red powder (25.2 mg, 67%). ^{1}H NMR (400 MHz, acetone-d_6) δ 10.11 (s, 2H), 7.60 (d, J = 7.9 Hz, 2H), 7.54 (s, 1H),

7.38 (d, J = 8.1 Hz, 2H), 7.24 (d, J = 2.3 Hz, 2H), 7.10–7.05 (m, 2H), 7.03–6.90 (m, 2H), 5.48 (s, 1H), 4.10 (q, J = 7.1 Hz, 2H), 3.97 (d, J = 5.9 Hz, 2H), 1.18 (t, J = 7.1 Hz, 3H); ^{13}C NMR (100 MHz, acetone-d_6) δ 173.6, 170.7, 137.6, 127.9, 124.7, 122.0, 119.9, 119.4, 115.1, 112.0, 61.2, 42.7, 41.9, 14.3.

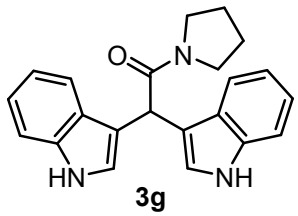

3g

2, 2-di(1H-indol-3-yl)-1-(pyrrolidin-1-yl)ethan-1-one (3g).[12] Pale red powder (20.9 mg, 61%). ^{1}H NMR (400 MHz, acetone-d_6) δ 10.10 (s, 2H), 7.66 (d, J = 8.0 Hz, 2H), 7.35 (d, J = 8.1 Hz, 2H), 7.18 (d, J = 2.3 Hz, 2H), 7.08–7.02 (m, 2H), 6.97–6.92 (m, 2H), 5.66 (s, 1H), 3.72 (t, J = 6.8 Hz, 2H), 3.45 (t, J = 6.8 Hz, 2H), 1.95–1.87 (m, 2H), 1.84–1.77 (m, 2H); ^{13}C NMR (100 MHz, acetone-d_6) δ 171.5, 137.6, 128.1, 124.7, 122.0, 120.0, 119.3, 115.3, 112.1, 47.4, 46.7, 40.0, 27.0, 25.0.

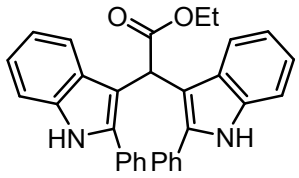

3h

Ethyl 2,2-bis(2-phenyl-1H-indol-3-yl)acetate (3h).[12] Pale yellow powder (42.3 mg, 90%). ^{1}H NMR (400 MHz, acetone-d_6) δ 10.50 (s, 2H), 7.51 (d, J = 7.4 Hz, 4H), 7.42 (t, J = 7.6 Hz, 4H), 7.36 (t, J = 7.4 Hz, 4H), 7.30 (d, J = 7.2 Hz, 2H), 7.07 (t, J = 7.6 Hz, 2H), 6.85 (t, J = 7.6 Hz, 2H), 5.65 (s, 1H), 3.99 (q, J = 7.1 Hz, 2H), 1.05 (t, J = 7.1 Hz, 3H); ^{13}C NMR (100 MHz, acetone-d_6) δ 174.1, 137.3, 137.1, 134.0, 129.4, 129.27, 129.26, 128.4, 122.3, 121.5, 119.9, 112.0, 110.8, 61.2, 42.7, 14.4.

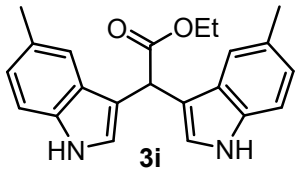

3i

Ethyl 2,2-bis(5-methyl-1H-indol-3-yl)acetate (3i).[12] Yellow powder (31.5 mg, 91%). ^{1}H NMR (400 MHz, $CDCl_3$) δ 7.91 (s, 2H), 7.42 (s, 2H), 7.19 (d, J = 8.3 Hz, 2H), 7.00 (dd, J = 8.3, 1.2 Hz, 2H), 6.96 (d, J = 2.1 Hz, 2H), 5.43 (s, 1H), 4.21 (q, J = 7.1 Hz, 2H), 2.41 (s, 6H), 1.27 (d, J = 7.1 Hz, 3H); ^{13}C NMR (100 MHz, $CDCl_3$) δ 173.6, 134.6, 128.7, 126.8, 123.7, 123.5, 118.9, 113.1, 110.9, 61.0, 40.5, 21.5, 14.2.

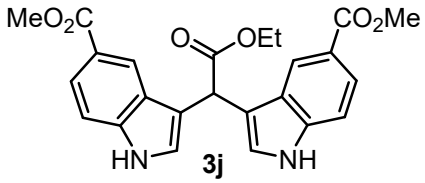

3j

Dimethyl 3,3'-(2-ethoxy-2-oxoethane-1,1-diyl)bis(1H-indole-5-carboxylate) (3j).[12] Yellow powder (19.1 mg, 44%). ^{1}H NMR (400 MHz, acetone-d_6) δ 10.57 (s, 2H), 8.48–8.45 (m, 2H), 7.82 (dd, J = 8.6, 1.6 Hz, 2H), 7.50 (d, J = 8.6 Hz, 2H), 7.40 (d, J = 1.9 Hz, 2H), 5.66 (s, 1H), 4.21 (q, J = 7.1 Hz, 2H), 3.84 (s, 6H), 1.26 (t, J = 7.1 Hz, 3H); ^{13}C NMR (100 MHz, acetone-d_6) δ 173.3, 168.2, 140.4, 127.3, 126.5, 123.6, 123.0, 122.1, 115.3, 112.2, 61.5, 51.9, 41.6, 14.5.

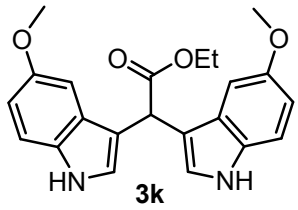

3k

Ethyl 2,2-bis(5-methoxy-1H-indol-3-yl)acetate (3k).[12] Yellow powder (22.7 mg, 60%). ^{1}H NMR (400 MHz, acetone-d_6) δ 10.02 (s, 2H), 7.29 (d, J = 8.8 Hz, 2H), 7.24 (d, J = 2.4 Hz, 2H), 7.15 (d, J = 2.3 Hz, 2H), 6.76 (dd, J = 8.8, 2.4 Hz, 2H), 5.44 (s, 1H), 4.18 (q, J = 7.1 Hz, 2H), 3.74 (s, 6H), 1.24 (t, J = 7.1 Hz, 3H); ^{13}C NMR (100 MHz, acetone-d_6) δ 173.8, 154.6, 132.7, 128.1, 125.1, 113.7, 112.8, 112.3, 101.6, 61.1, 55.6, 41.5, 14.6.

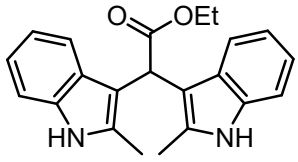

3l

Ethyl 2, 2-bis(2-methyl-1H-indol-3-yl)acetate (3l).[12] Yellow powder (31.5 mg, 91%). ^{1}H NMR (400 MHz, $CDCl_3$) δ 7.81 (s, 2H), 7.39 (d, J = 7.9 Hz, 2H), 7.20 (d, J = 8.0 Hz, 2H), 7.09–7.02 (m, 2H), 7.01–6.95 (m, 2H), 5.43 (s, 1H), 4.26 (q, J = 7.1 Hz, 2H), 2.14 (s, 6H), 1.24 (t, J = 7.2 Hz, 3H); ^{13}C NMR (100 MHz, $CDCl_3$) δ 173.7, 134.8, 132.2, 128.2, 120.8, 119.3, 118.7, 110.2, 108.6, 61.0, 40.0, 14.2, 12.3.

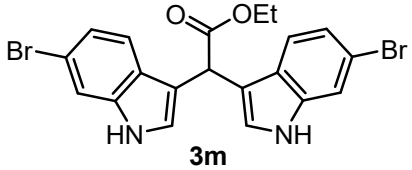

3m

Ethyl 2,2-bis(6-bromo-1H-indol-3-yl)acetate (3m).[12] Yellow powder (35.7 mg, 75%). ^{1}H NMR (400 MHz, acetone-d_6) δ 10.35 (s, 2H), 7.61 (d, J = 1.5 Hz, 2H), 7.55 (d, J =

8.5 Hz, 2H), 7.32 (dd, J = 2.4, 0.7 Hz, 2H), 7.12 (dd, J = 8.5, 1.8 Hz, 2H), 5.49 (s, 1H), 4.17 (q, J = 7.1 Hz, 2H), 1.21 (t, J = 7.1 Hz, 3H); ^{13}C NMR (100 MHz, acetone-d_6) δ 173.3, 138.5, 126.7, 125.6, 122.7, 121.7, 115.4, 115.1, 114.1, 61.4, 41.4, 14.5.

General procedure for the visible-light induced aerobic oxidative synthesis of benzothiazoles catalyzed by TPA-MP-1.

To a solution of 2-aminothiophenol **4** (0.1 mmol, 1 eq), aldehyde **5** (0.12 mmol, 1.2 eq) in EtOH (1.0 mL) were added TPA-MP-1 (7.5 mg, 5 mol%). The mixed solution was irradiated with a 24 W blue LED under an air atmosphere at room temperature. After the completion of the reaction as monitored by TLC, the solvent was removed under vacuum, and the residue was separated by silica gel column chromatography (with petroleum ether/EtOAc = 4/1 as an eluent) to afford the product **6**.

Table S2 Control experiments[a]

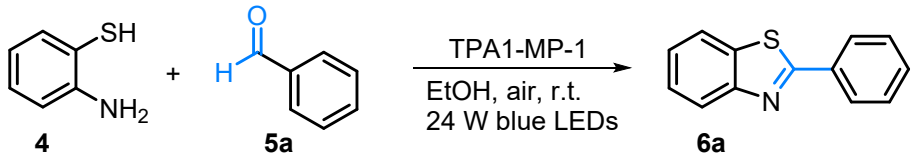

4 **5a** **6a**

Entry	Catalyst	Additive	Yield (%)[b]
1	—	—	51
2	TPA1	—	55
3[c]	TPA-MP-1	—	trace
4[d]	TPA-MP-1	—	trace
5	TPA-MP-1	TEMPO	trace
6	TPA-MP-1	KI	56
7	TPA-MP-1	$CuSO_4$	37
8	TPA-MP-1	*p*-benzoquinone	21
9	TPA-MP-1	NaN_3	20

[a] 2-aminothiophenol **4** (0.1 mmol), aldehyde **5a** (0.12 mmol), TPA-MP-1 (5 mol%), additive (1.5 eq), and EtOH (1.0 mL) was placed in a 5 mL flask and irradiated with a 24 W blue LED under an air atmosphere at room temperature. [b] Yield of isolated product. [c] Reaction was carried out under Ar. [d] Reaction was carried out in the dark.

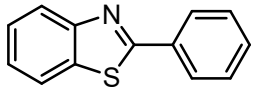

6a

2-Phenylbenzo[d]thiazole (6a).[13] White solid (18.1 mg, 86%). ^{1}H NMR (400 MHz, $CDCl_3$) δ 8.11–8.07 (m, 3H), 7.89 (d, J = 1.2 Hz, 1H), 7.51–7.47(m, 4H), 7.40–7.36 (m, 1H); ^{13}C NMR (100 MHz, $CDCl_3$) δ 168.1, 154.1, 135.1, 133.6, 130.9, 129.0, 127.6, 126.3, 125.2, 123.2, 121.6.

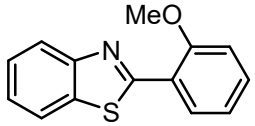

6b

2-(2-Methoxyphenyl)benzo[d]thiazole (6b).[14] White solid (23.8 mg, 99%). ^{1}H NMR (400 MHz, $CDCl_3$) δ 8.54 (dd, J = 7.9, 1.8 Hz, 1H), 8.10 (d, J = 8.2 Hz, 1H), 7.93 (d, J = 7.8 Hz, 1H), 7.54–7.43 (m, 2H), 7.39–7.35 (m, 1H), 7.16–7.12 (m, 1H), 7.08 (d, J = 8.8 Hz, 1H), 4.06 (s, 3H); ^{13}C NMR (100 MHz, $CDCl_3$) δ 163.1, 157.2, 152.1, 136.1, 131.7, 129.5, 125.9, 124.6, 122.8, 122.3, 121.18, 121.16, 111.7, 55.7.

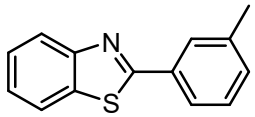

6c

2-(m-Tolyl)benzo[d]thiazole (6c).[13] White solid (18.0 mg, 80%). ^{1}H NMR (400 MHz, $CDCl_3$) δ 8.08 (d, J = 8.2 Hz, 1H), 7.95 (s, 1H), 7.92–7.85(m, 2H), 7.52–7.47 (m, 1H), 7.41–7.36(m, 2H), 7.31 (d, J = 7.7 Hz, 1H), 2.46 (s, 3H); ^{13}C NMR (100 MHz, $CDCl_3$) δ 168.3, 154.1, 138.9, 135.0, 133.5, 131.8, 128.9, 128.0, 126.3, 125.1, 124.9, 123.2, 121.6, 21.3.

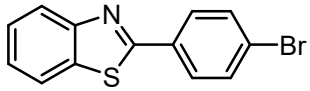

6d

2-(4-Bromophenyl)benzo[d]thiazole (6d).[15] White solid (24.6 mg, 85%). ^{1}H NMR (400 MHz, $CDCl_3$) δ 8.07 (d, J = 8.1 Hz, 1H), 7.98–7.93 (m, 2H), 7.90 (d, J = 7.3 Hz, 1H), 7.64–7.60 (m, 2H), 7.52–7.48 (m, 1H), 7.42–7.37 (m,1H); ^{13}C NMR (100 MHz, $CDCl_3$) δ 166.7, 154.0, 135.0, 132.5, 132.2, 128.9, 126.5, 125.4, 123.3, 121.6.

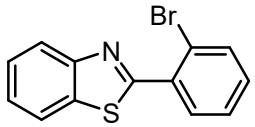

6e

***2-(2-Bromophenyl)benzo[d]thiazole (6e)*.**[14] White solid (26.7 mg, 92%). ^{1}H NMR (400 MHz, $CDCl_3$) δ 8.15 (d, J = 8.2 Hz, 1H), 8.00 (dd, J = 7.8, 1.8 Hz, 1H), 7.95 (d, J = 7.9 Hz, 1H), 7.74 (dd, J = 8.1, 1.3 Hz, 1H), 7.54–7.51 (m, 1H), 7.47–7.42 (m, 2H), 7.33 (td, J = 7.7, 1.8 Hz, 1H); ^{13}C NMR (100 MHz, $CDCl_3$) δ 165.6, 152.7, 136.1, 134.5, 134.1, 132.2, 131.2, 127.6, 126.3, 125.5, 123.6, 122.1, 121.4.

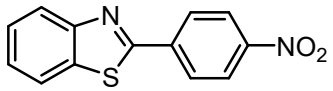

6f

***2-(4-Nitrophenyl)benzo[d]thiazole (6f)*.**[16] Yellow solid (7.9 mg, 31%). ^{1}H NMR (400 MHz, $CDCl_3$) δ 8.38–8.33 (m, 2H), 8.30–8.25 (m, 2H), 8.13 (d, J = 8.2 Hz, 1H), 7.96 (d, J = 8.0 Hz, 1H), 7.59–7.53 (m, 1H), 7.49–7.44 (m, 1H); ^{13}C NMR (100 MHz, $CDCl_3$) δ 164.8, 154.1, 149.0, 139.2, 135.5, 128.2, 126.9, 126.2, 124.3, 123.9, 121.8.

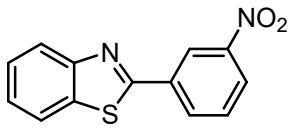

6g

***2-(3-Nitrophenyl)benzo[d]thiazole (6g)*.**[17] White solid (17.4 mg, 68%). ^{1}H NMR (400 MHz, $CDCl_3$) δ 8.93–8.92 (m, 1H), 8.43–8.40 (m, 1H), 8.34–8.31 (m, 1H), 8.11 (d, J = 8.2 Hz, 1H), 7.92 (d, J = 8.4 Hz, 1H), 7.68 (t, J = 8.0 Hz, 1H), 7.58–7.52(m, 1H), 7.47–7.43 (m, 1H); ^{13}C NMR (100 MHz, $CDCl_3$) δ 164.9, 153.9, 148.7, 135.3, 135.2, 133.0, 130.1, 126.8, 126.0, 125.1, 123.7, 122.3, 121.8.

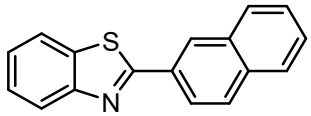

6h

***2-(Naphthalen-2-yl)benzo[d]thiazole (6h)*.**[13] White solid (24.0 mg, 92%). ^{1}H NMR (400 MHz, $CDCl_3$) δ 8.57 (d, J = 1.4 Hz, 1H), 8.22 (dd, J = 8.5, 1.8 Hz, 1H), 8.12 (d, J = 8.2 Hz, 1H), 8.00–7.85 (m, 4H), 7.58–7.49 (m, 3H), 7.43–7.39 (m, 1H); ^{13}C NMR (100 MHz, $CDCl_3$) δ 168.1, 154.2, 135.1, 134.6, 133.2, 131.0, 128.8, 127.9, 127.6, 127.5, 126.9, 126.4, 125.2, 124.4, 123.2, 121.6.

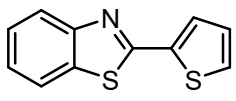

6i

***2-(Thiophen-2-yl)benzo[d]thiazole (6i)*.**[13] White solid (16.3 mg, 60%). ^{1}H NMR (400 MHz, $CDCl_3$) δ 8.04 (d, J = 8.3 Hz, 1H), 7.83 (d, J = 7.8 Hz, 1H), 7.64 (dd, J = 3.7, 1.2 Hz, 1H), 7.52–7.42 (m, 2H), 7.38–7.34 (m, 1H), 7.12 (dd, J = 5.0, 3.7 Hz, 1H); ^{13}C

NMR (100 MHz, $CDCl_3$) δ 161.4, 153.7, 137.3, 134.7, 129.3, 128.6, 128.0, 126.4, 125.2, 123.0, 121.4.

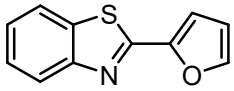

6j

2-(Furan-2-yl)benzo[d]thiazole (6j).[16] White solid (13.7 mg, 87%). ^{1}H NMR (400 MHz, $CDCl_3$) δ 8.04 (d, J = 8.0 Hz, 1H), 7.84 (d, J = 8.0 Hz, 1H), 7.56 (d, J = 1.7 Hz, 1H), 7.48–7.43 (m,1H), 7.36–7.31 (m, 1H), 7.17 (d, J = 3.5 Hz, 1H), 6.55 (dd, J = 3.5, 1.8 Hz, 1H); ^{13}C NMR (100 MHz, $CDCl_3$) δ 157.4, 153.6, 148.6, 144.5, 134.1, 126.3, 125.0, 123.0, 121.4, 112.4, 111.3.

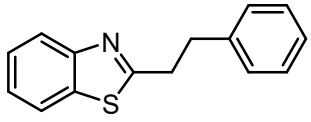

6k

2-Phenethylbenzo[d]thiazole (6k).[16] White solid (19.1 mg, 80%). ^{1}H NMR (400 MHz, $CDCl_3$) δ 7.99 (d, J = 8.2 Hz, 1H), 7.83 (d, J = 8.2 Hz, 1H), 7.49–7.43(m, 1H), 7.38–7.19 (m, 6H), 3.47–3.39 (m, 2H), 3.25–3.15 (m, 2H); ^{13}C NMR (100 MHz, $CDCl_3$) δ 170.9, 153.2, 140.2, 135.1, 128.6, 128.4, 126.4, 125.9, 124.7, 122.6, 121.5, 36.0, 35.5.

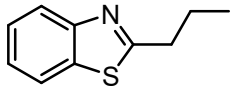

6l

2-Propylbenzo[d]thiazole (6l).[15] Yellow oil (7.6 mg, 43%). ^{1}H NMR (400 MHz, $CDCl_3$) δ 7.97 (d, J = 8.2 Hz, 1H), 7.82 (d, J = 7.9 Hz, 1H), 7.46–7.40 (m, 1H), 7.35–7.30 (m, 1H), 3.08 (t, J = 7.4 Hz, 2H), 1.91 (h, J = 7.4 Hz, 2H), 1.05 (t, J = 7.4 Hz, 3H); ^{13}C NMR (100 MHz, $CDCl_3$) δ 172.1, 153.2, 135.1, 125.8, 124.5, 122.4, 121.4, 36.2, 23.0, 13.7.

H. Quantum Yield Measurement

A solution of ferrioxalate was chosen as actinometer following the procedure described by the IUPAC (subcommittee on photochemistry).[18] The procedure is based on the decomposition under irradiation of ferric ions to ferrous ions which are complexed by 1,10-phenanthroline. This photochemical transformation has a known quantum yield and the complexation of $Fe^{2+}$with 1,10-phenanthroline can be monitored by UV-Visible absorption since its extinction coefficient at 510 nm is known (=11100 $M^{-1}cm^{-1}$). Therefore, the moles of iron-phenanthroline complex formed are related to moles of photons absorbed.0.006 M, 0.012 M, or 0.15 M solutions of ferrioxalate can be used for actinometry. In this case we chose a concentration of 0.15 M. The solutions were prepared and stored in a dark laboratory as follows:

Potassium ferrioxalate solution 0.15 M: 1.84 g of $K_3[Fe(C_2O_4)_3]\cdot 3H_2O$ and 1.75 mL of H_2SO_4 were added into a 25 mL volumetric flack and filled to the mark with ultrapure water.

1,10-phenanthroline 0.01 M: 100 mg of 1,10-phenantroline monohydrate were added to 50 mL volumetric flask and filled to the mark with ultrapure water.

Buffer solution: 2.5 g of NaOAc and 0.25 mL of H_2SO_4 were added to 25 mL volumetric flask and filled to the mark with ultrapure water.

Model reaction solution: **1a** (0.1 mmol, 1.0 eq), **2a** (0.21 mmol, 2.1 eq), citric acid (1.5 eq) and TPA-MP-1 (5 mol%) were added to an oven-dried 3 mL quartz cuvette (l = 1 cm) equipped with a magnetic stir bar and a plastic plug in CH_3CN (2 mL) under argon atmosphere.

Actinometry procedure:

(1) 2 mL of potassium ferrioxalate solutions (0.15M) were added to a quartz cuvette under dark conditions while being stirred. Then, the actinometry solutions were irradiated with 405 nm LED for specified time intervals (0, 15, 30, 45, 60 s) and a 0.1 mL aliquot was taken.

(2) 4 mL of buffer solution and 1 mL of 0.01 M 1,10-phenanthroline were added to each aliquot, and the final volume was raised to 10 mL with ultrapure water. All samples were stored in the dark and stirred for one hour.

(3) The absorbance spectrum of each sample was monitored at 510 nm for each time interval by the UV-2600 spectrometer. The absorbance to each time was related with the photochemically produced Fe^{2+} ions across the Lambert-Beer Law (Equation [1]):

$$\text{moles } Fe^{2+} = \frac{V_1 \cdot V_3 \cdot \Delta A(510\ nm)}{V_2 \cdot l \cdot \varepsilon(510\ nm)} \qquad [1]$$

where V_1 is the irradiated volume (2 mL), V_2 is the aliquot of the irradiated solution taken for the determination of the ferrous ions (0.1 mL), V_3 is the final volume after complexation with phenanthroline (10 mL), l is the optical path-length of the irradiation quartz cuvette (1 cm), ΔA (510 nm) the optical difference in absorbance between the irradiated solution and that taken in the dark, ε (510 nm) is the extinction coefficient of the complex $Fe(phen)_3^{2+}$(11100 $M^{-1}cm^{-1}$).

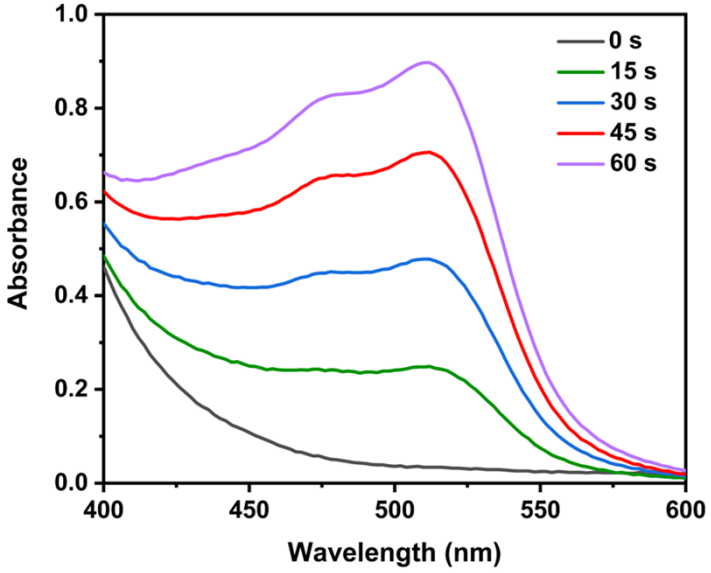

Fig S12 The absorbance spectrum of each time interval.

(4) The moles of Fe^{2+}formed (x) are plotted as a function of time (t) (Fig. S13). The slope of the line (*dx/dt*) was correlated to the moles of incident photons by unit of time (*qn,p*) using the following equation [2]:

$$q_{n,p} = \frac{dx/dt}{\Phi(\lambda) \cdot f}, \quad f = [1-10^{-A(\lambda)}] \qquad [2]$$

Where Φ (λ) is the quantum yield of the actinometer reaction at the irradiated wavelength, in this case being 1.14 at 405 nm.[19] The value of the photon flux must be divided by the fraction of absorbed light f at the irradiation wavelength and A (λ) is the absorbance of the actinometer solution (ferrioxalate) at the irradiated wavelength (405 nm) obtaining a value of 4.2, f = 1. Therefore, the moles of incident photons by unit of time was determined as 2.28×10^{-7} einstein s^{-1}.

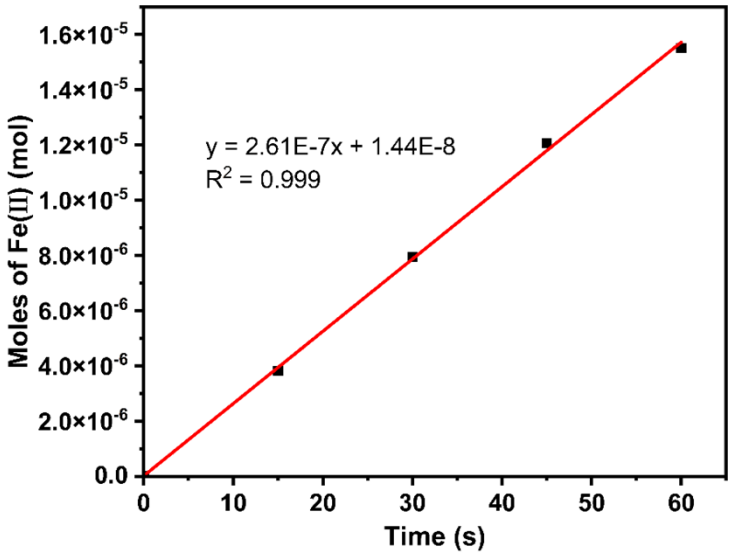

Fig. S13 The moles of Fe^{2+} formed (x) are plotted as a function of time (t).

(5) The kinetics of the reaction under study were done as irradiating the actinometer solution described above. The model reaction solutions were irradiated using the same spectrometer with consecutive measurements every half hour. The moles of product (**3a**) formed were determined by ^{1}H-NMR spectrum in DMSO-d_6. Plotting the moles of product versus the irradiation time, the slope *dx/dt* can be related with the quantum yield across the equation [2] being equal to $(qn,p) \times \Phi(\lambda) \times (1\text{-}10^{-A(\lambda)})$. **The quantum yield at 405 nm of reaction photocatalized by TPA-MP-1 were calculated as 0.016.**

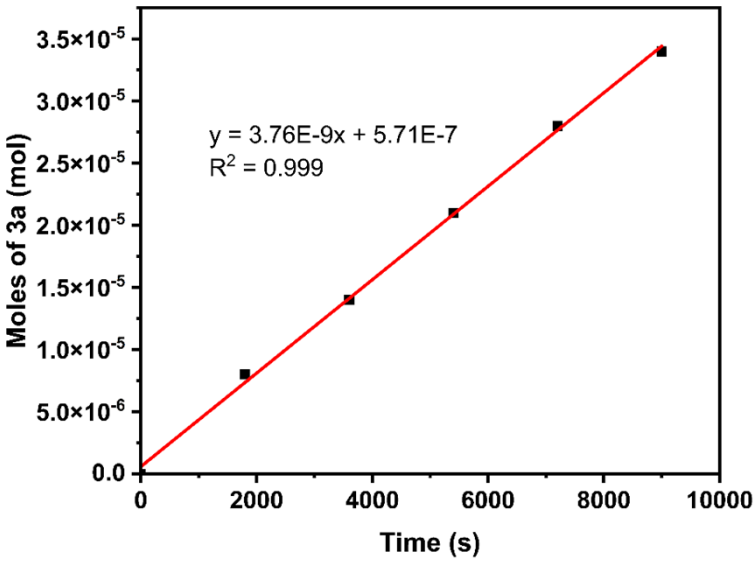

Fig. S14 Plotting the moles of product versus the irradiation time.

I. References

1. J. Xie and Z.-Z. Huang, *Angew. Chem., Int. Ed.*, 2010, **49**, 10181.
2. L. Zhao, O. Basle and C.-J. Li, *Proc. Natl. Acad. Sci. U. S. A.*, 2009, **106**, 4106.
3. Y. Sun, N. Zhou, W. Zhang, Y. Li, Z. Cheng, J. Zhu, Z. Zhang and X. Zhu, *J. Polym. Sci. Pol. Chem.*, 2012, **50**, 3788.
4. M. Faccini, M. Balakrishnan, M. B. J. Diemeer, Z.-P. Hu, K. Clays, I. Asselberghs, A. Leinse, A. Driessen, D. N. Reinhoudt and W. Verboom, *J. Mater. Chem.*, 2008, **18**, 2141.
5. S. J. G. Linkletter, G. A. Pearson and R. I. Walter, *J. Am. Chem. Soc.*, 1977, **99**, 5269.
6. Y. Meng, D. Gu, F. Zhang, Y. Shi, H. Yang, Z. Li, C. Yu, B. Tu and D. Zhao, *Angew. Chem., Int. Ed.,* 2005, **44**, 7053.
7. M. J. Frisch, G. W. Trucks, H. B. Schlegel, G. E. Scuseria, M. A. Robb, J. R. Cheeseman, G. Scalmani, V. Barone, B. Mennucci, G. A. Petersson, H. Nakatsuji, M. Caricato, X. Li, H. P. Hratchian,A. F. Izmaylov, J. Bloino, G. Zheng, J. L. Sonnenberg, M. Hada,M. Ehara, K. Toyota, R. Fukuda, J. Hasegawa, M. Ishida, T. Nakajima,Y. Honda, O. Kitao, H. Nakai, T. Vreven, J. A. Montgomery, Jr.,J. E. Peralta, F. Ogliaro, M. Bearpark, J. J. Heyd, E. Brothers,K. N. Kudin, V. N. Staroverov, T. Keith, R. Kobayashi, J. Normand,K. Raghavachari, A. Rendell, J. C. Burant, S. S. Iyengar, J. Tomasi,M. Cossi, N. Rega, J. M. Millam, M. Klene, J. E. Knox, J. B. Cross,V. Bakken, C. Adamo, J. Jaramillo, R. Gomperts, R. E. Stratmann,O. Yazyev, A. J. Austin, R. Cammi, C. Pomelli, J. W. Ochterski,R. L. Martin, K. Morokuma, V. G. Zakrzewski, G. A. Voth,P. Salvador, J. J. Dannenberg, S. Dapprich, A. D. Daniels,O. Farkas, J. B. Foresman, J. V. Ortiz, J. Cioslowski,and D. J. Fox, Gaussian 09, D.01, Gaussian, Inc., Wallingford CT, 2013.
8. Parr, R. G.; Yang, W. *Density-functional Theory of Atoms and Molecules*; Oxford University Press: New York, 1989.
9. (a) A. D. Becke, *J. Chem. Phys.* 1993, **98**, 5648; (b) C. Lee, W. Yang, R. G. Parr *Phys. Rev. B* 1988, **37**, 785.
10. C. Y. Legault, CYLVIEW, 1.0b, Université de Sherbrooke, **2009**; http://www.cylview.org.
11. M. Kou, Y. Wang, Y. Xu, L. Ye, Y. Huang, B. Jia, H. Li, J. Ren, Y. Deng, J. Chen, Y. Zhou, K. Lei, L. Wang, W. Liu, H. Huang and T. Ma. *Angew. Chem. Int. Ed.*

2022**, 61**, e202200413.

12. Y. Zhang, X. Yang, H. Zhou, S. Li, Y. Zhu and Y. Li, *Org. Chem. Front.*, 2018, **5**, 2120.
13. Y. Huang, D. Yan, X. Wang, P. Zhou, W. Wu and H. Jiang, *Chem. Commun.,* 2018, **54**, 1742.
14. D. B. Lima, F. Penteado, M. M. Vieira, D. Alves, G. Perin, C. Santi and E. J. Lenardão, *Eur. J. Org. Chem.,* 2017, **26**, 3830.
15. H. Wang, Q. Wu, J.-D. Zhang, H.-Y. Li and H.-X. Li, *Org. Lett.*, 2021, **23**, 2078.
16. J. Zhang, X. Zhao, P. Liu and P. Sun, *J. Org. Chem.,* 2019, **84**, 12596.
17. Y. Liao, H. Qi, S. Chen, P. Jiang, W. Zhou and G.-J. Deng, *Org. Lett.,* 2012, **14**, 6004.
18. H. J. Kuhn, S. E. Braslavsky, R. Schmidt, *Pure Appl. Chem.* 2004, **76**, 2105.
19. M. Montalti, A. Credi, L. Prodi, M. T. Gandolfi, *Handbook of Photochemistry*, 3rd Ed; Taylor & Francis Group, LLC. Boca Raton, FL, 2006, 601–616.

J. Copies of ^{1}H and ^{13}C NMR Spectra

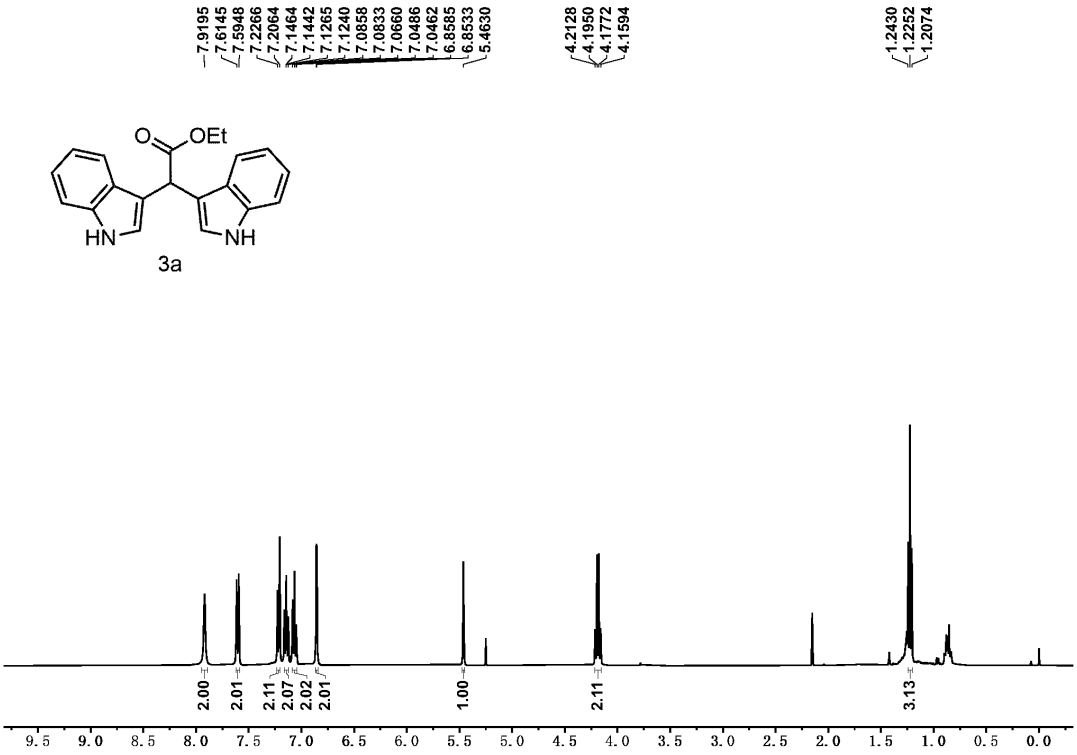

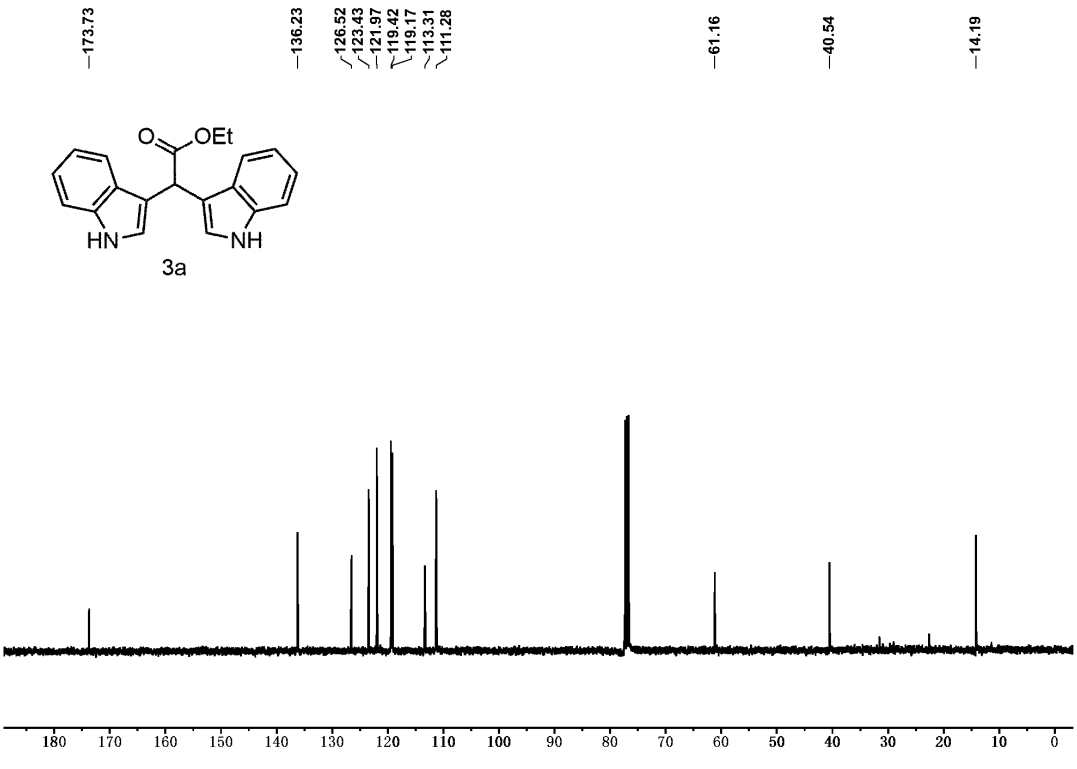

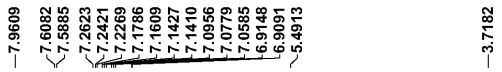
7.9609
7.6082
7.5885
7.2623
7.2421
7.2269
7.1786
7.1609
7.1427
7.1410
7.0956
7.0779
7.0585
6.9148
6.9091
5.4913
3.7182

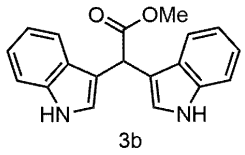
O
OMe
HN
NH

3b

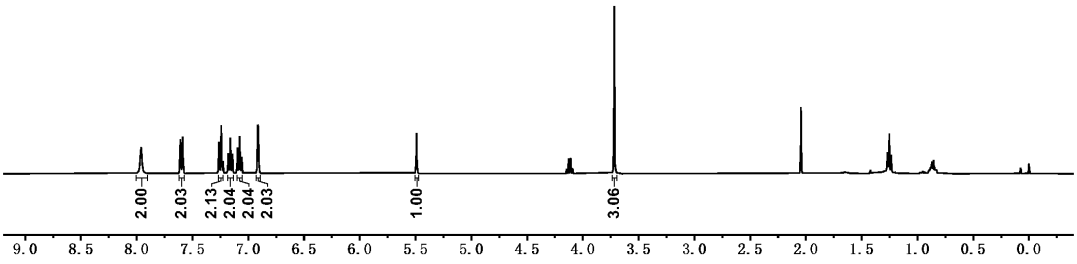
2.00
2.03
2.13
2.04
2.04
2.03
1.00
3.06
9.0
8.5
8.0
7.5
7.0
6.5
6.0
5.5
5.0
4.5
4.0
3.5
3.0
2.5
2.0
1.5
1.0
0.5
0.0

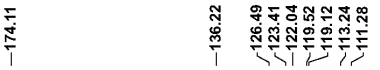
174.11
136.22
126.49
123.41
122.04
119.52
119.12
113.24
111.28
52.28
40.35

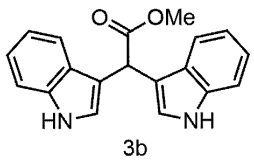
O
OMe
HN
NH

3b

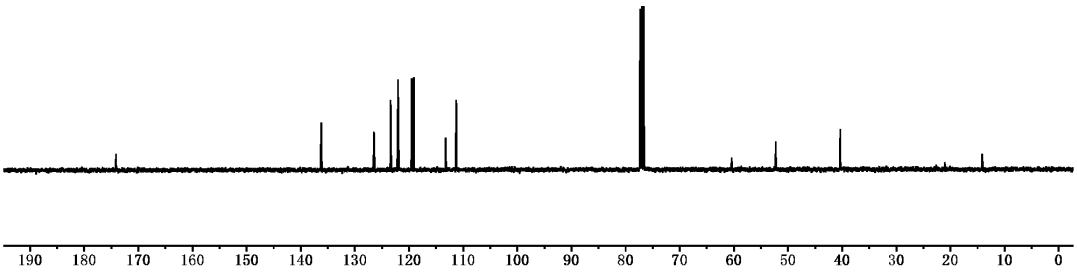
190
180
170
160
150
140
130
120
110
100
90
80
70
60
50
40
30
20
10
0

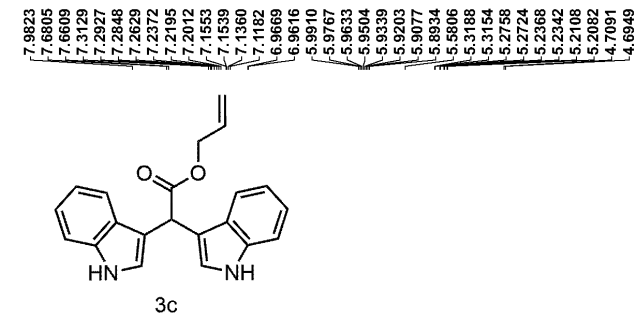
7.9823
7.6805
7.6609
7.3129
7.2927
7.2848
7.2629
7.2372
7.2195
7.2012
7.1553
7.1539
7.1360
7.1182
6.9669
6.9616
5.9910
5.9767
5.9633
5.9504
5.9339
5.9203
5.9077
5.8934
5.5806
5.3188
5.3154
5.2758
5.2724
5.2368
5.2342
5.2108
5.2082
4.7091
4.6949
O
O
HN
NH

3c

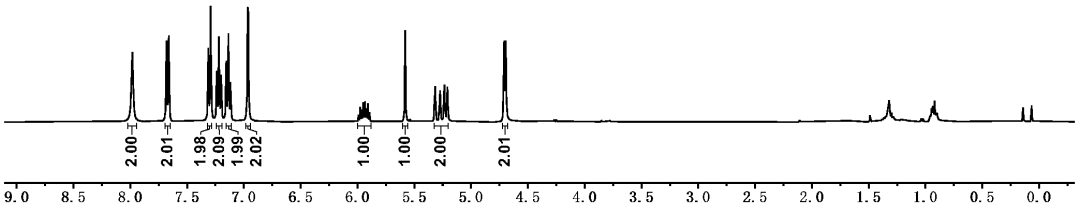
2.00
2.01
1.98
2.09
1.99
2.02
1.00
1.00
2.00
2.01
9.0
8.5
8.0
7.5
7.0
6.5
6.0
5.5
5.0
4.5
4.0
3.5
3.0
2.5
2.0
1.5
1.0
0.5
0.0

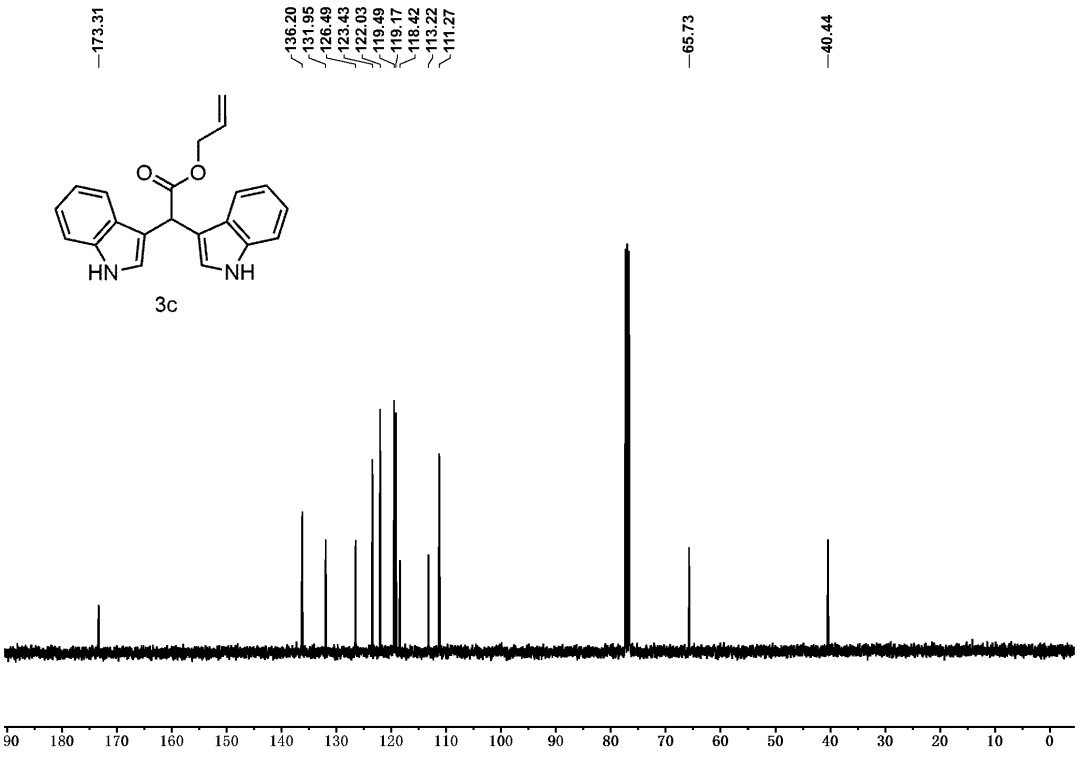
173.31
136.20
131.95
126.49
123.43
122.03
119.49
119.17
118.42
113.22
111.27
65.73
40.44
O
O
HN
NH
90
180
170
160
150
140
130
120
110
100
90
80
70
60
50
40
30
20
10
0

3c


10.1741
7.6359
7.6160
7.4148
7.3944
7.3416
7.3361
7.3310
7.3209
7.3165
7.3092
7.3051
7.2990
7.2876
7.2813
7.2751
7.1199
7.1175
7.0998
7.0820
7.0796
6.9988
6.9966
6.9789
6.9612
6.9591
5.6174
5.2046

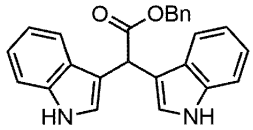
O
OBn
HN
NH

3d

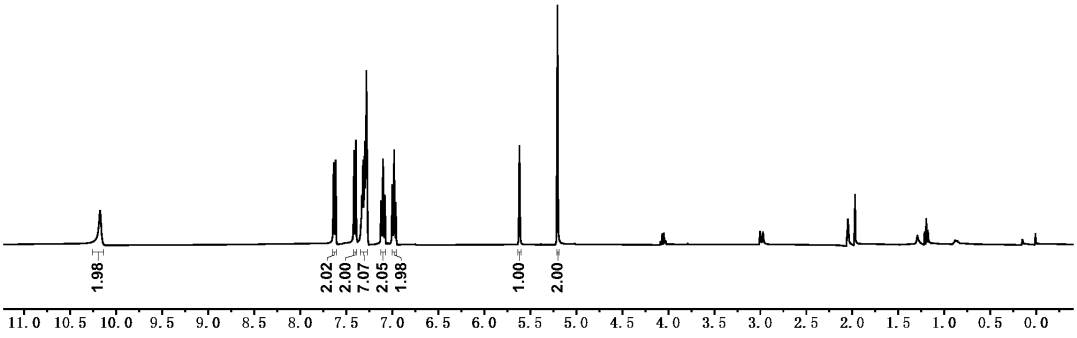
1.98
2.02
2.00
7.07
2.05
1.98
1.00
2.00
11.0 10.5 10.0 9.5 9.0 8.5 8.0 7.5 7.0 6.5 6.0 5.5 5.0 4.5 4.0 3.5 3.0 2.5 2.0 1.5 1.0 0.5 0.0


173.58
137.67
137.40
129.15
128.85
128.71
127.73
124.56
122.23
119.97
119.61
113.91
112.22
66.85
41.55

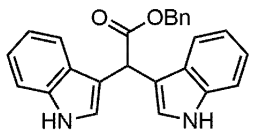
O
OBn
HN
NH

3d

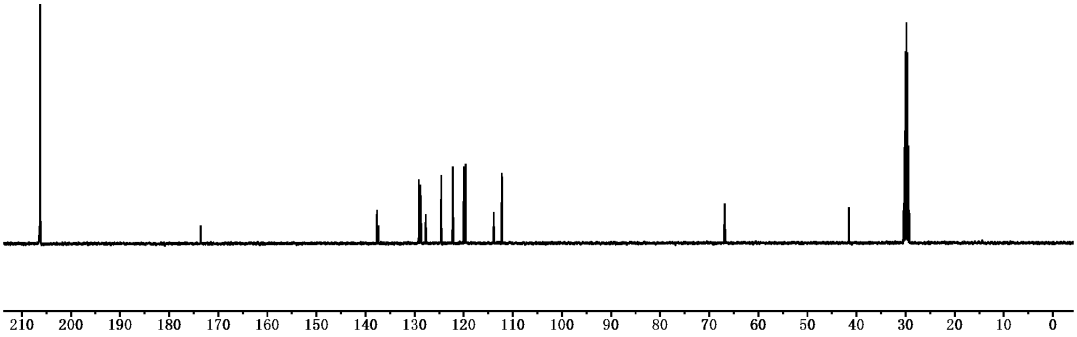
210 200 190 180 170 160 150 140 130 120 110 100 90 80 70 60 50 40 30 20 10 0

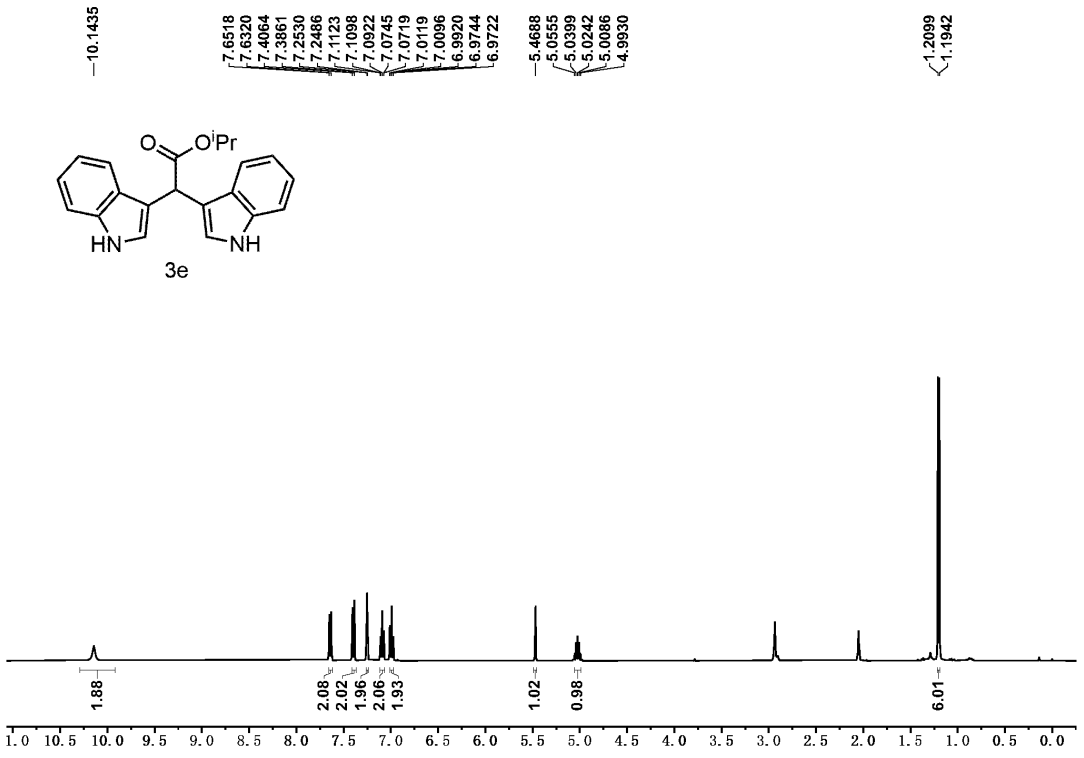
10.1435
7.6518
7.6320
7.4064
7.3861
7.2530
7.2486
7.1123
7.1098
7.0922
7.0745
7.0719
7.0119
7.0096
6.9920
6.9744
6.9722
5.4688
5.0555
5.0399
5.0242
5.0086
4.9930
1.2099
1.1942
O
OiPr
HN
NH
3e
1.88
2.08
2.02
1.96
2.06
1.93
1.02
0.98
6.01

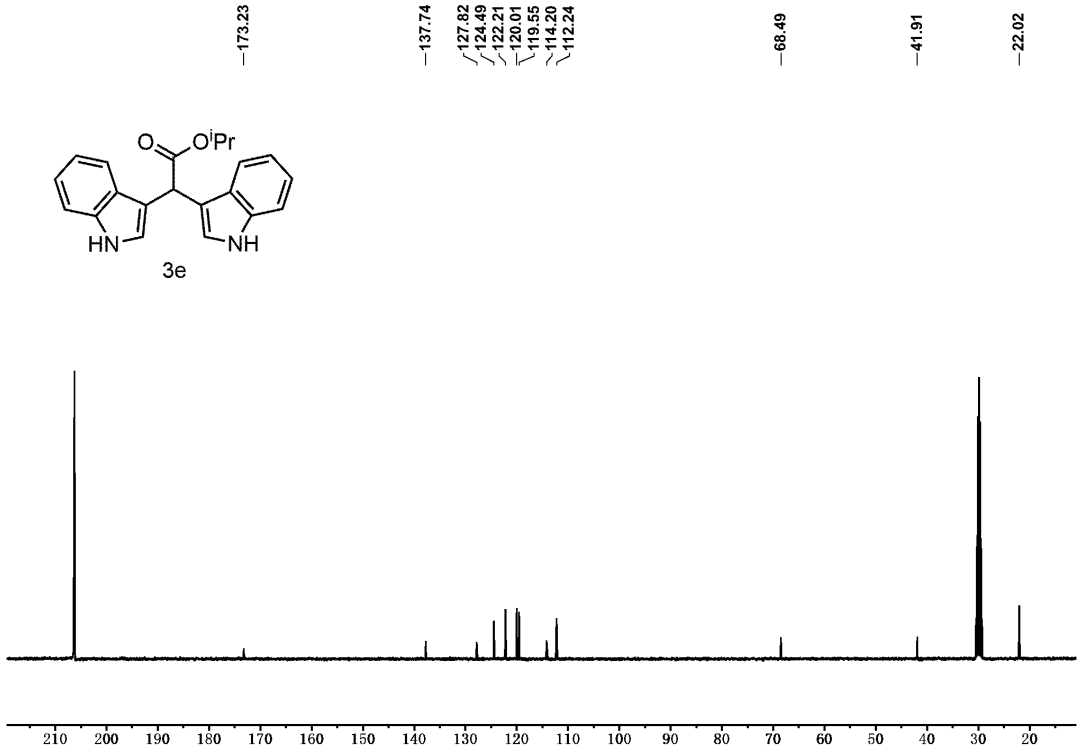
173.23
137.74
127.82
124.49
122.21
120.01
119.55
114.20
112.24
68.49
41.91
22.02
O
OiPr
HN
NH
3e

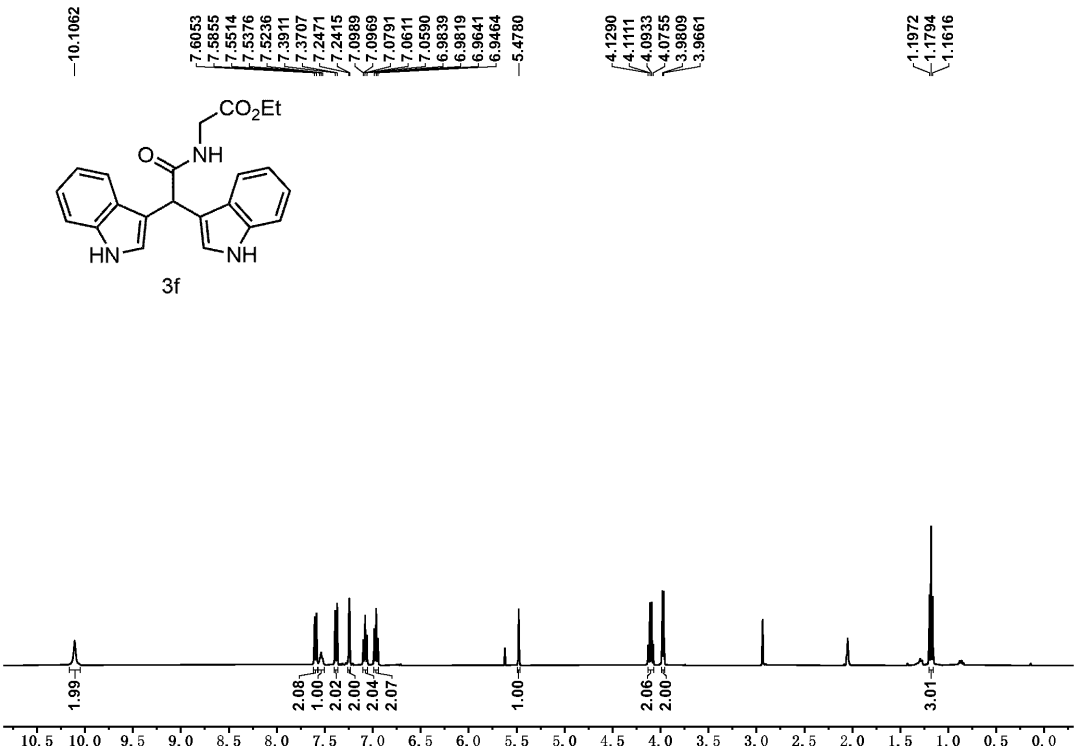
10.1062
7.6053
7.5855
7.5514
7.5376
7.5236
7.3911
7.3707
7.2471
7.2415
7.0989
7.0969
7.0791
7.0611
7.0590
6.9839
6.9819
6.9641
6.9464
5.4780
4.1290
4.1111
4.0933
4.0755
3.9809
3.9661
1.1972
1.1794
1.1616
CO2Et
O
NH
HN
NH
3f
1.99
2.08
1.00
2.02
2.00
2.04
2.07
1.00
2.06
2.00
3.01
10.5 10.0 9.5 9.0 8.5 8.0 7.5 7.0 6.5 6.0 5.5 5.0 4.5 4.0 3.5 3.0 2.5 2.0 1.5 1.0 0.5 0.0

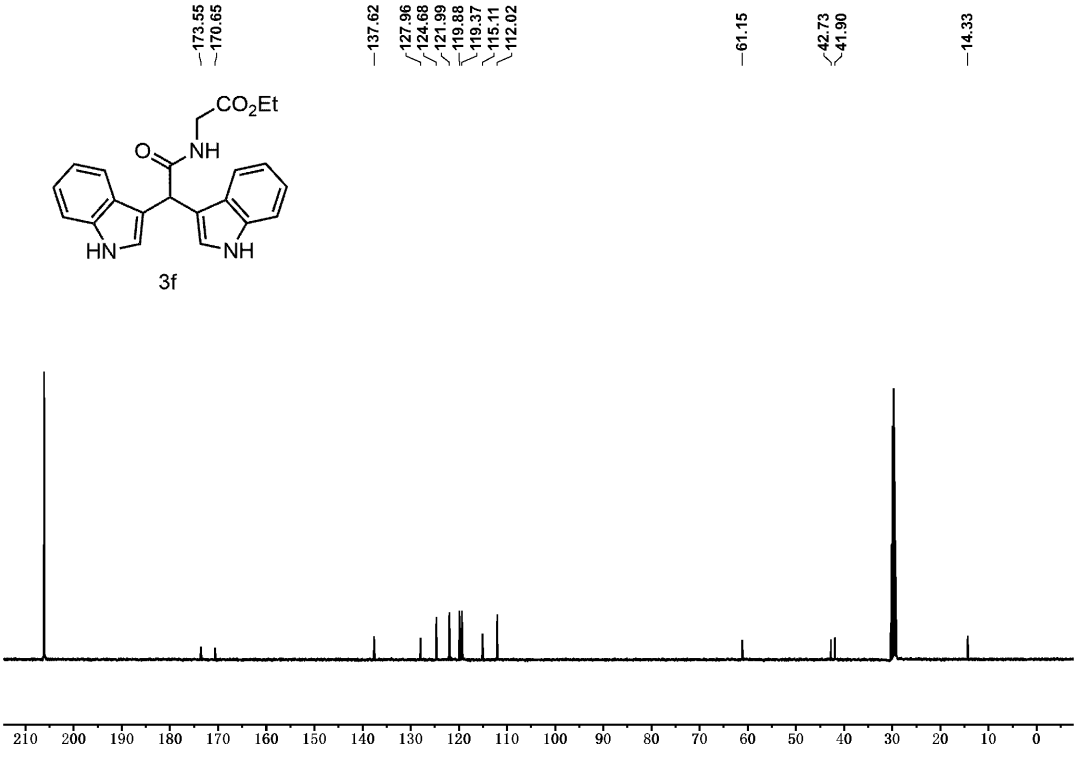
173.55
170.65
137.62
127.96
124.68
121.99
119.88
119.37
115.11
112.02
61.15
42.73
41.90
14.33
CO2Et
O
NH
HN
NH
3f
210 200 190 180 170 160 150 140 130 120 110 100 90 80 70 60 50 40 30 20 10 0

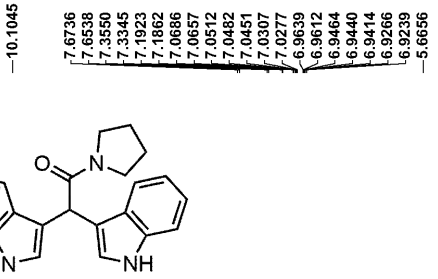
10.1045
7.6736
7.6538
7.3550
7.3345
7.1923
7.1862
7.0686
7.0657
7.0512
7.0482
7.0451
7.0307
7.0277
6.9639
6.9612
6.9464
6.9440
6.9414
6.9266
6.9239
5.6656
3.7355
3.7187
3.7017
3.4720
3.4548
3.4378
1.9399
1.9372
1.9232
1.9203
1.9047
1.8879
1.8724
1.8700
1.8376
1.8351
1.8211
1.8179
1.8031
1.7872
1.7840
1.7699
1.7669

O
N
HN
NH

3g

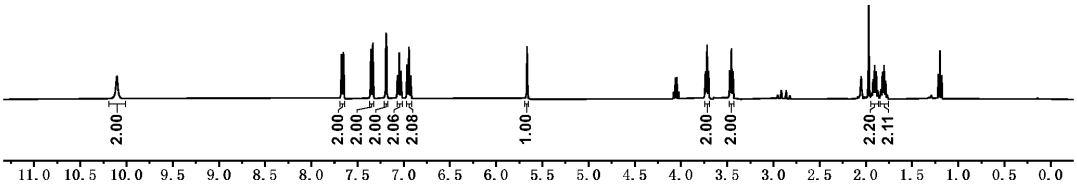
2.00
2.00
2.00
2.06
2.08
1.00
2.00
2.00
2.20
2.11
11.0 10.5 10.0 9.5 9.0 8.5 8.0 7.5 7.0 6.5 6.0 5.5 5.0 4.5 4.0 3.5 3.0 2.5 2.0 1.5 1.0 0.5 0.0

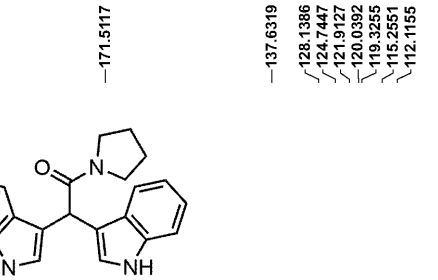
171.5117
137.6319
128.1386
124.7447
121.9127
120.0392
119.3255
115.2551
112.1155
47.3899
46.6987
40.0077
26.9099
24.9542

O
N
HN
NH

3g

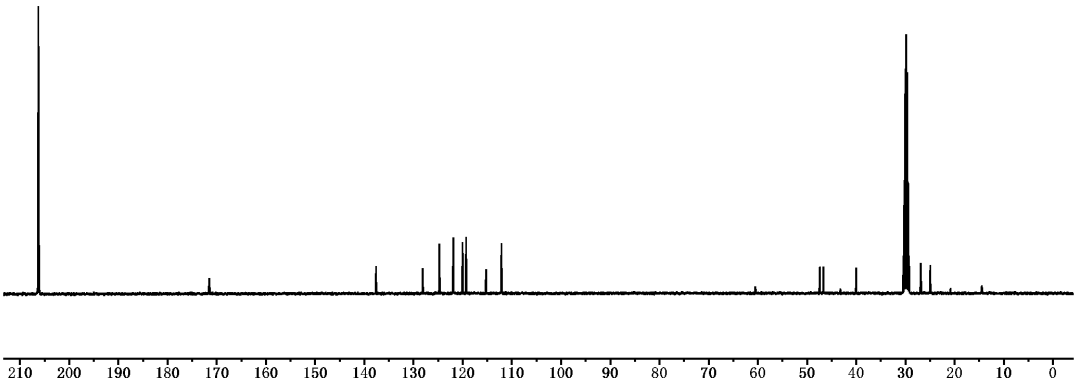
210 200 190 180 170 160 150 140 130 120 110 100 90 80 70 60 50 40 30 20 10 0

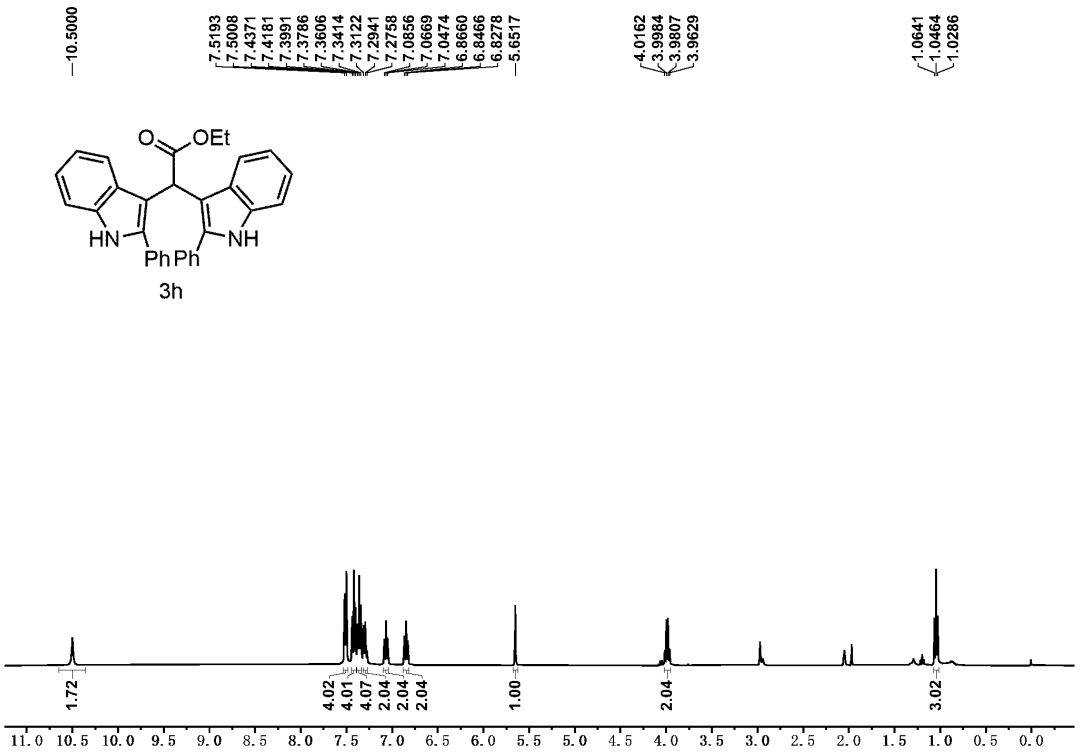
10.5000
7.5193
7.5008
7.4371
7.4181
7.3991
7.3786
7.3606
7.3414
7.3122
7.2941
7.2758
7.0856
7.0669
7.0474
6.8660
6.8466
6.8278
5.6517
4.0162
3.9984
3.9807
3.9629
1.0641
1.0464
1.0286
O
OEt
HN
NH
Ph
Ph
3h
1.72
4.02
4.01
4.07
2.04
2.04
2.04
1.00
2.04
3.02
11.0 10.5 10.0 9.5 9.0 8.5 8.0 7.5 7.0 6.5 6.0 5.5 5.0 4.5 4.0 3.5 3.0 2.5 2.0 1.5 1.0 0.5 0.0

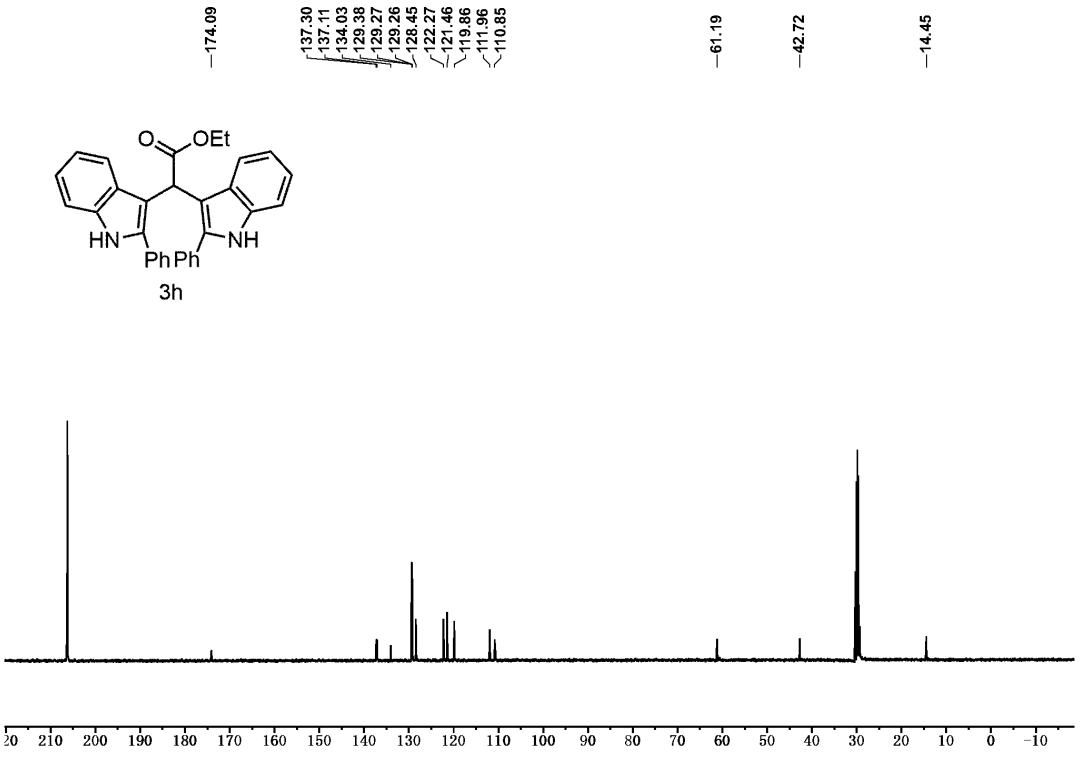
174.09
137.30
137.11
134.03
129.38
129.27
129.26
128.45
122.27
121.46
119.86
111.96
110.85
61.19
42.72
14.45
O
OEt
HN
NH
Ph
Ph
3h
210 200 190 180 170 160 150 140 130 120 110 100 90 80 70 60 50 40 30 20 10 0 -10

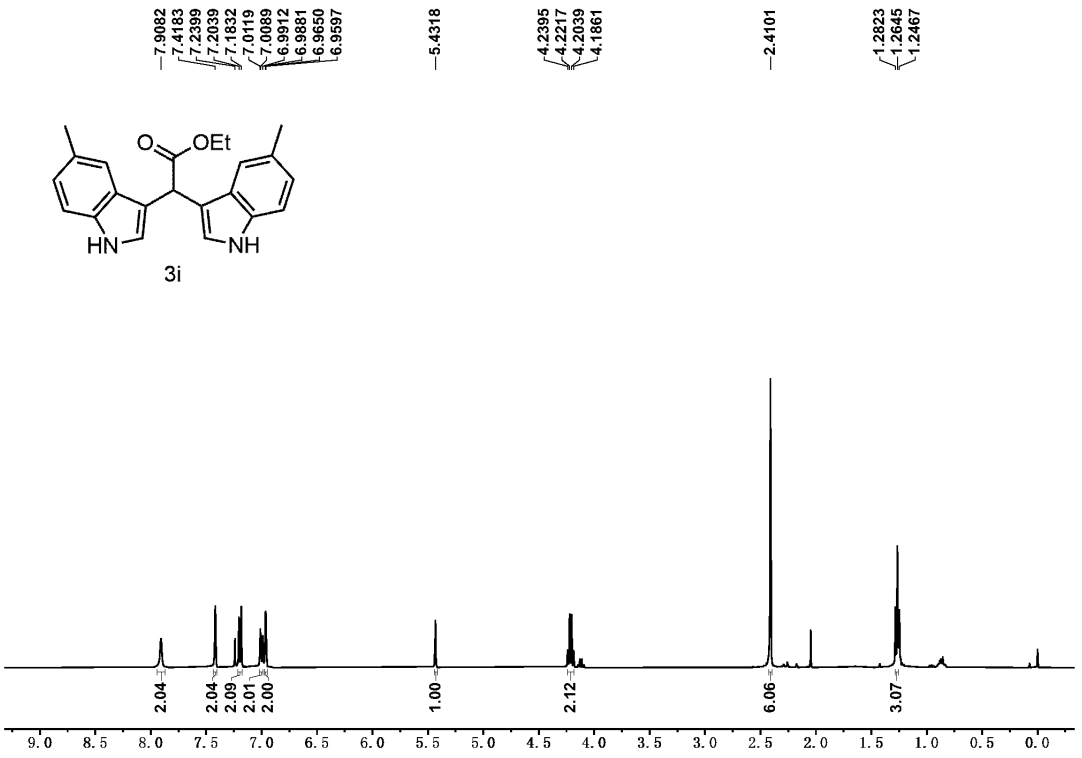
7.9082
7.4183
7.2399
7.2039
7.1832
7.0119
7.0089
6.9912
6.9881
6.9650
6.9597
5.4318
4.2395
4.2217
4.2039
4.1861
2.4101
1.2823
1.2645
1.2467
O
OEt
HN
NH
3i
2.04
2.04
2.09
2.01
2.00
1.00
2.12
6.06
3.07
9.0
8.5
8.0
7.5
7.0
6.5
6.0
5.5
5.0
4.5
4.0
3.5
3.0
2.5
2.0
1.5
1.0
0.5
0.0

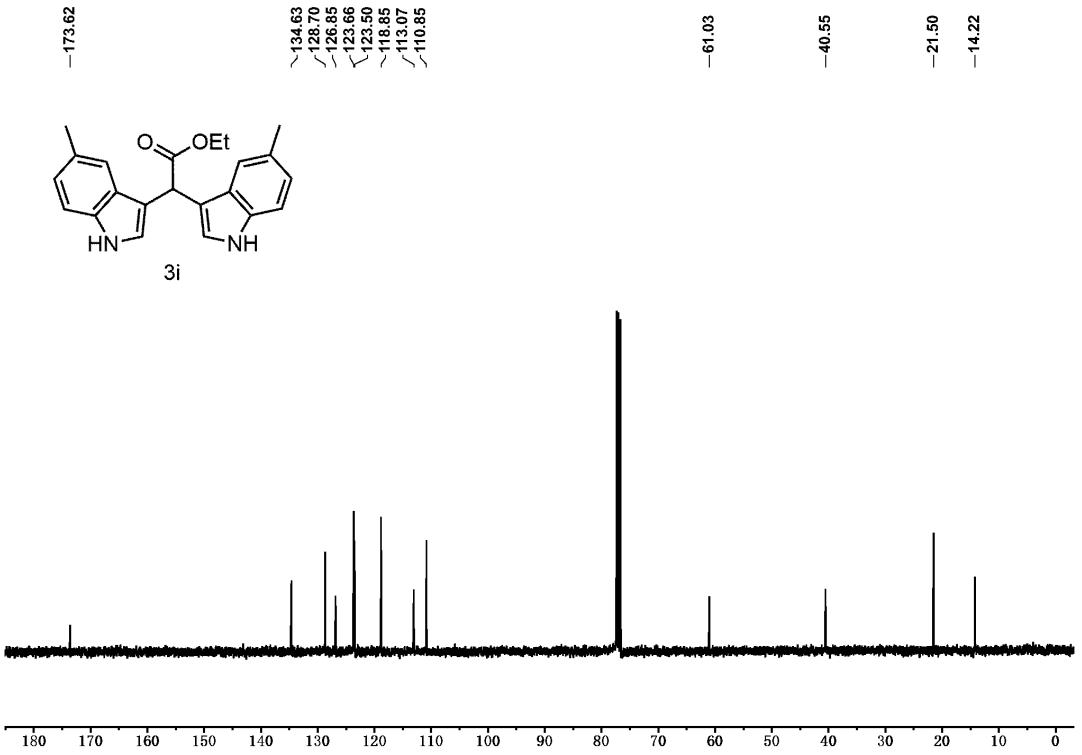
173.62
134.63
128.70
126.85
123.66
123.50
118.85
113.07
110.85
61.03
40.55
21.50
14.22
O
OEt
HN
NH
3i
180
170
160
150
140
130
120
110
100
90
80
70
60
50
40
30
20
10
0

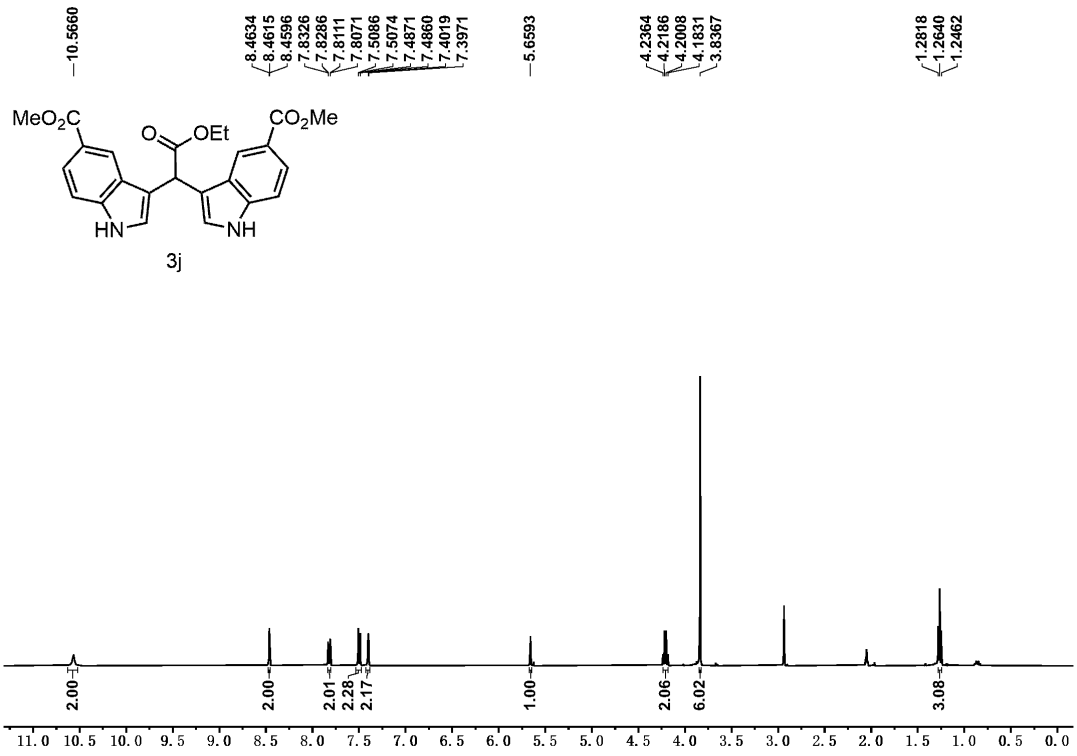
10.5660
8.4634
8.4615
8.4596
7.8326
7.8286
7.8111
7.8071
7.5086
7.5074
7.4871
7.4860
7.4019
7.3971
5.6593
4.2364
4.2186
4.2008
4.1831
3.8367
1.2818
1.2640
1.2462
MeO2C
O
OEt
CO2Me
HN
NH
3j
2.00
2.00
2.01
2.28
2.17
1.00
2.06
6.02
3.08
11.0 10.5 10.0 9.5 9.0 8.5 8.0 7.5 7.0 6.5 6.0 5.5 5.0 4.5 4.0 3.5 3.0 2.5 2.0 1.5 1.0 0.5 0.0

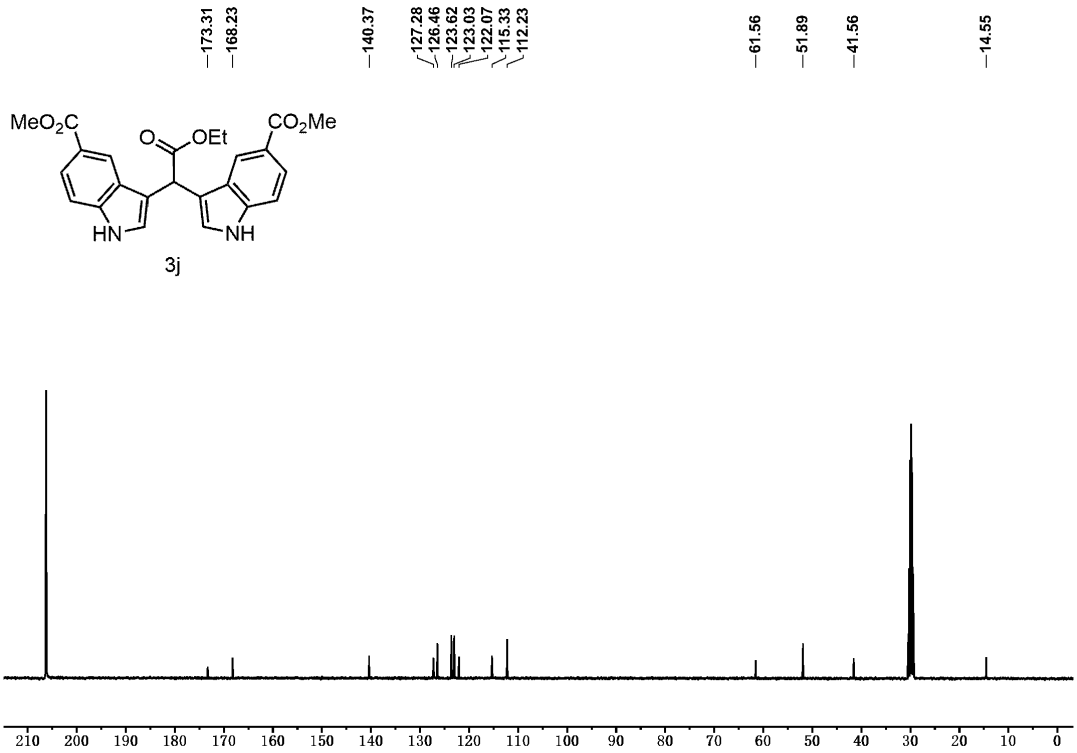
173.31
168.23
140.37
127.28
126.46
123.62
123.03
122.07
115.33
112.23
61.56
51.89
41.56
14.55
MeO2C
O
OEt
CO2Me
HN
NH
3j
210 200 190 180 170 160 150 140 130 120 110 100 90 80 70 60 50 40 30 20 10 0

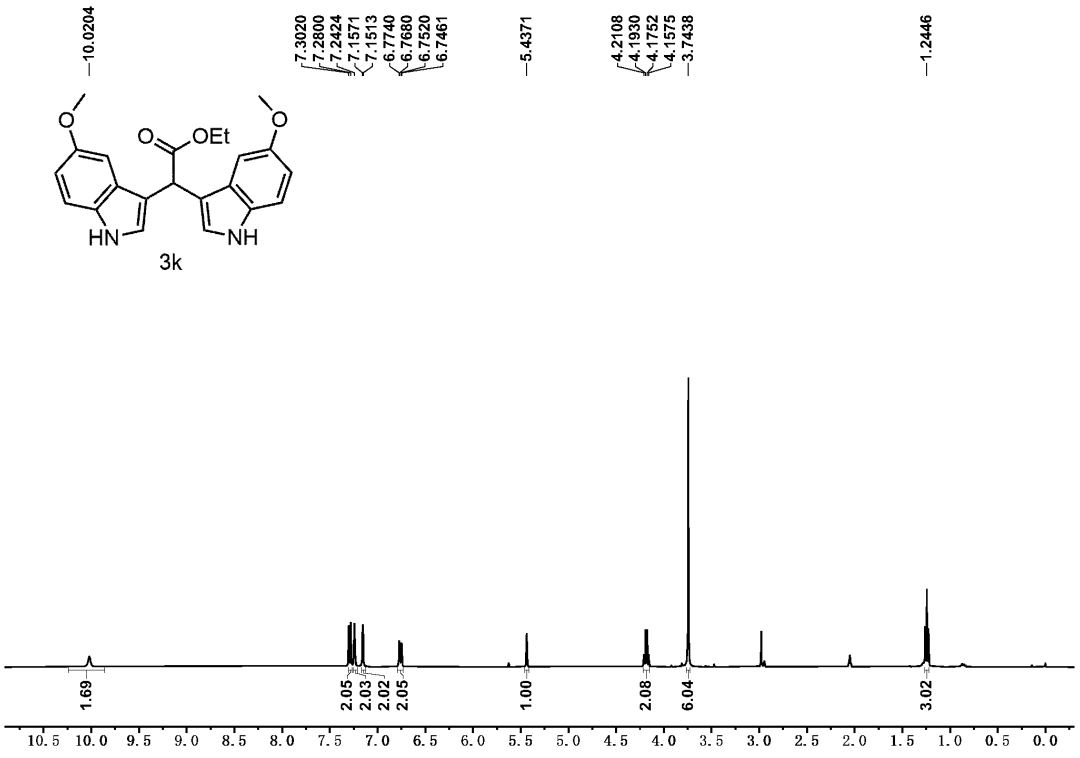
10.0204
7.3020
7.2800
7.2424
7.1571
7.1513
6.7740
6.7680
6.7520
6.7461
5.4371
4.2108
4.1930
4.1752
4.1575
3.7438
1.2446
O
OEt
O
HN
NH
3k
1.69
2.05
2.03
2.02
2.05
1.00
2.08
6.04
3.02
10.5 10.0 9.5 9.0 8.5 8.0 7.5 7.0 6.5 6.0 5.5 5.0 4.5 4.0 3.5 3.0 2.5 2.0 1.5 1.0 0.5 0.0

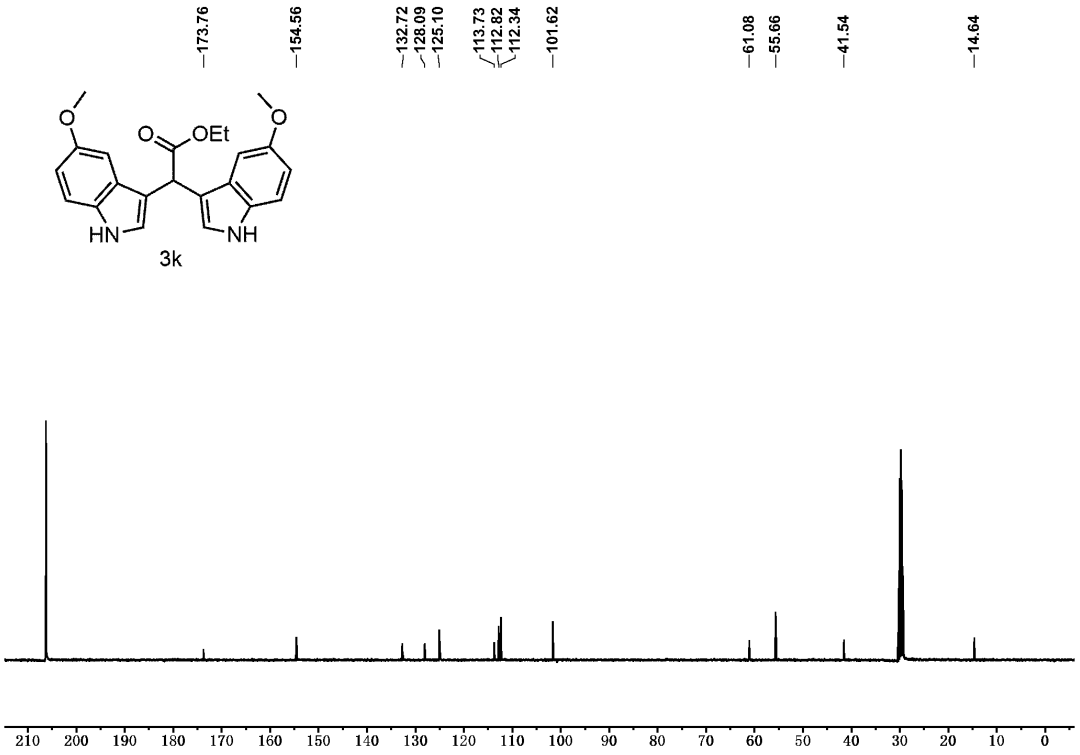
173.76
154.56
132.72
128.09
125.10
113.73
112.82
112.34
101.62
61.08
55.66
41.54
14.64
O
OEt
O
HN
NH
3k
210 200 190 180 170 160 150 140 130 120 110 100 90 80 70 60 50 40 30 20 10 0

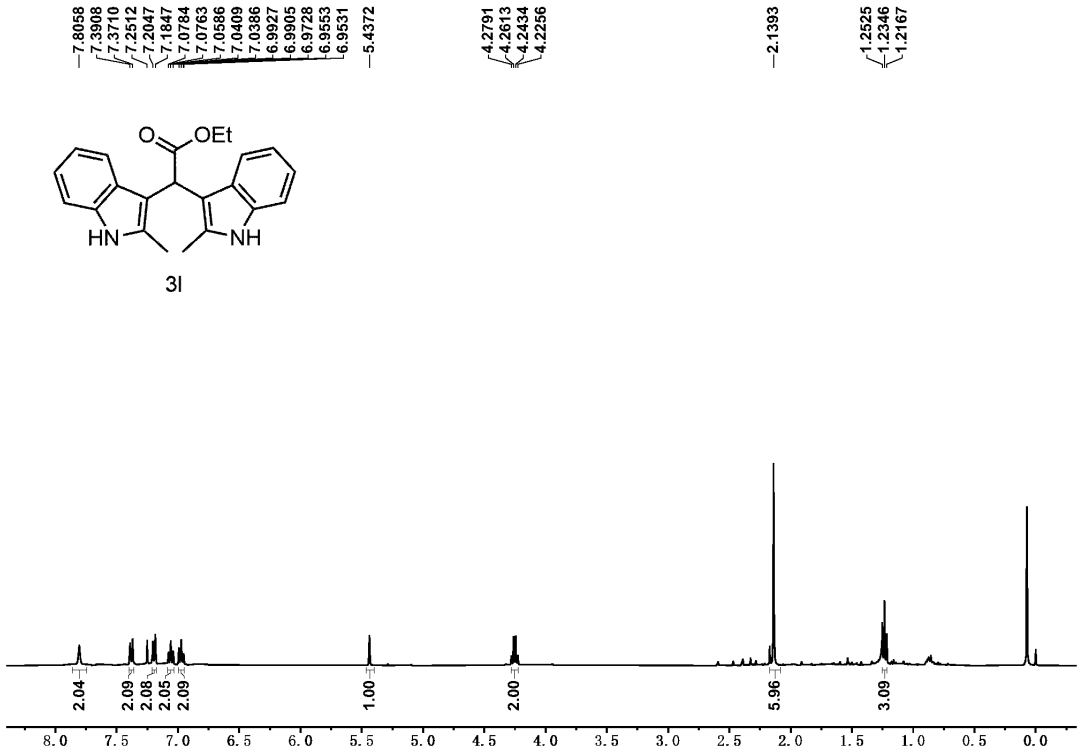
7.8058
7.3908
7.3710
7.2512
7.2047
7.1847
7.0784
7.0763
7.0586
7.0409
7.0386
6.9927
6.9905
6.9728
6.9553
6.9531
5.4372
4.2791
4.2613
4.2434
4.2256
2.1393
1.2525
1.2346
1.2167
O
OEt
HN
NH
3l
2.04
2.09
2.08
2.05
2.09
1.00
2.00
5.96
3.09
8.0
7.5
7.0
6.5
6.0
5.5
5.0
4.5
4.0
3.5
3.0
2.5
2.0
1.5
1.0
0.5
0.0

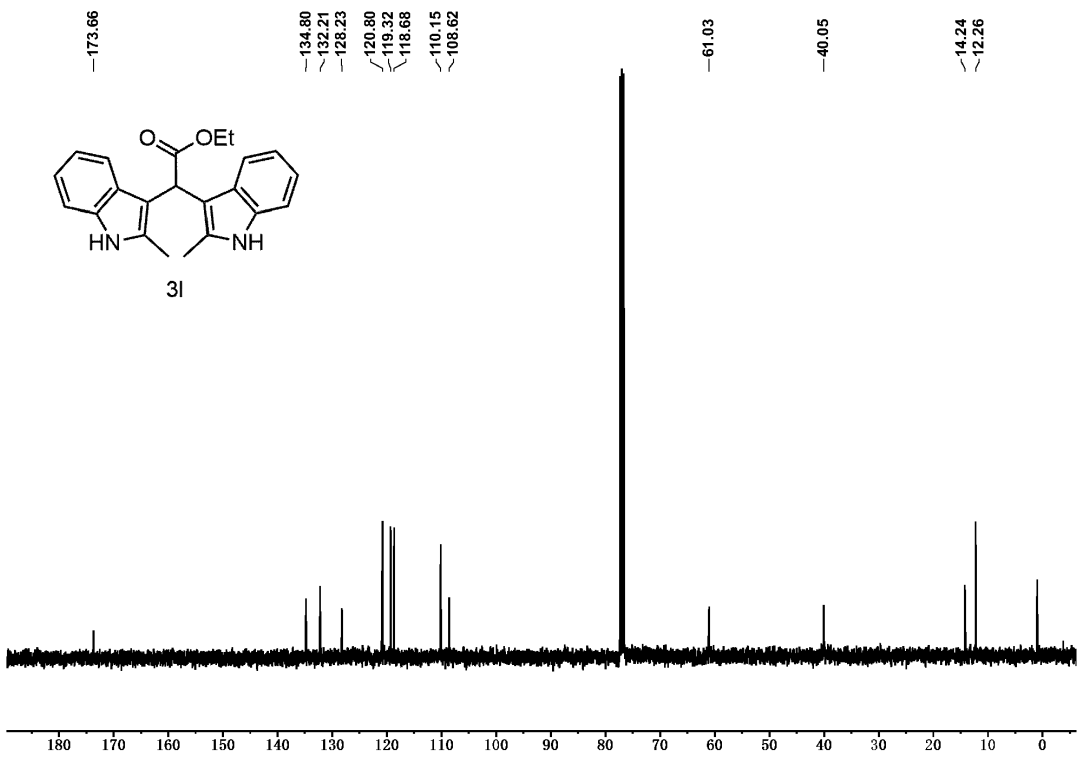
173.66
134.80
132.21
128.23
120.80
119.32
118.68
110.15
108.62
61.03
40.05
14.24
12.26
O
OEt
HN
NH
3l
180
170
160
150
140
130
120
110
100
90
80
70
60
50
40
30
20
10
0

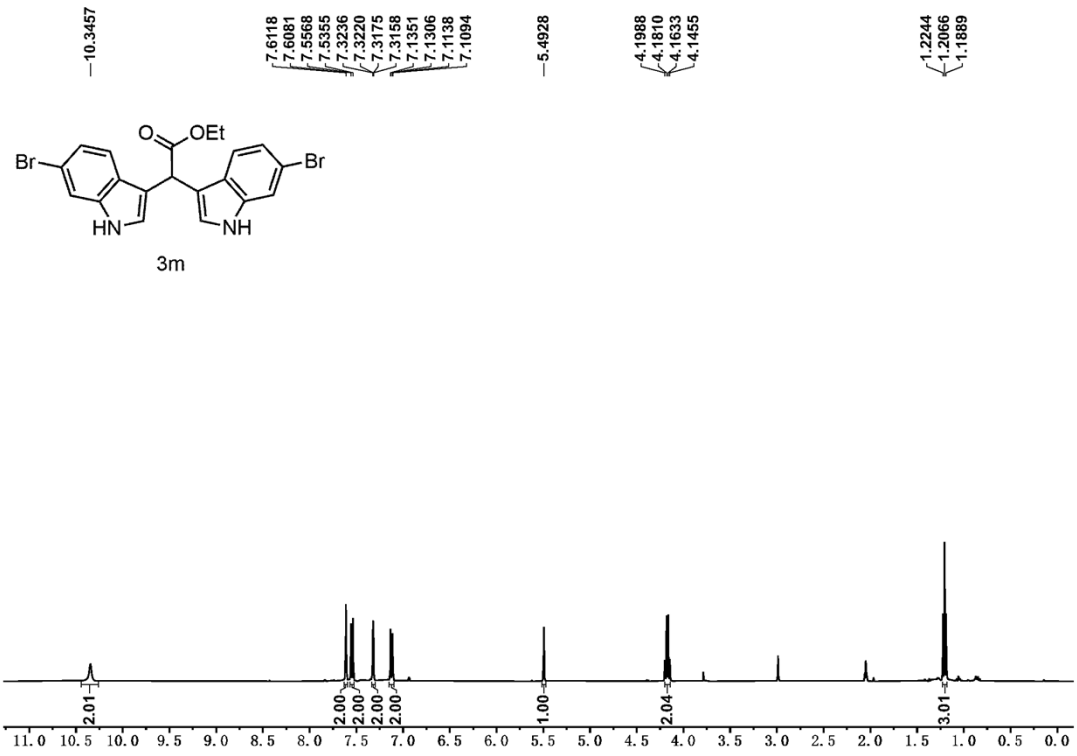
10.3457
7.6118
7.6081
7.5568
7.5355
7.3236
7.3220
7.3175
7.3158
7.1351
7.1306
7.1138
7.1094
5.4928
4.1988
4.1810
4.1633
4.1455
1.2244
1.2066
1.1889
O
OEt
Br
Br
HN
NH
3m
2.01
2.00
2.00
2.00
2.00
1.00
2.04
3.01
11.0 10.5 10.0 9.5 9.0 8.5 8.0 7.5 7.0 6.5 6.0 5.5 5.0 4.5 4.0 3.5 3.0 2.5 2.0 1.5 1.0 0.5 0.0

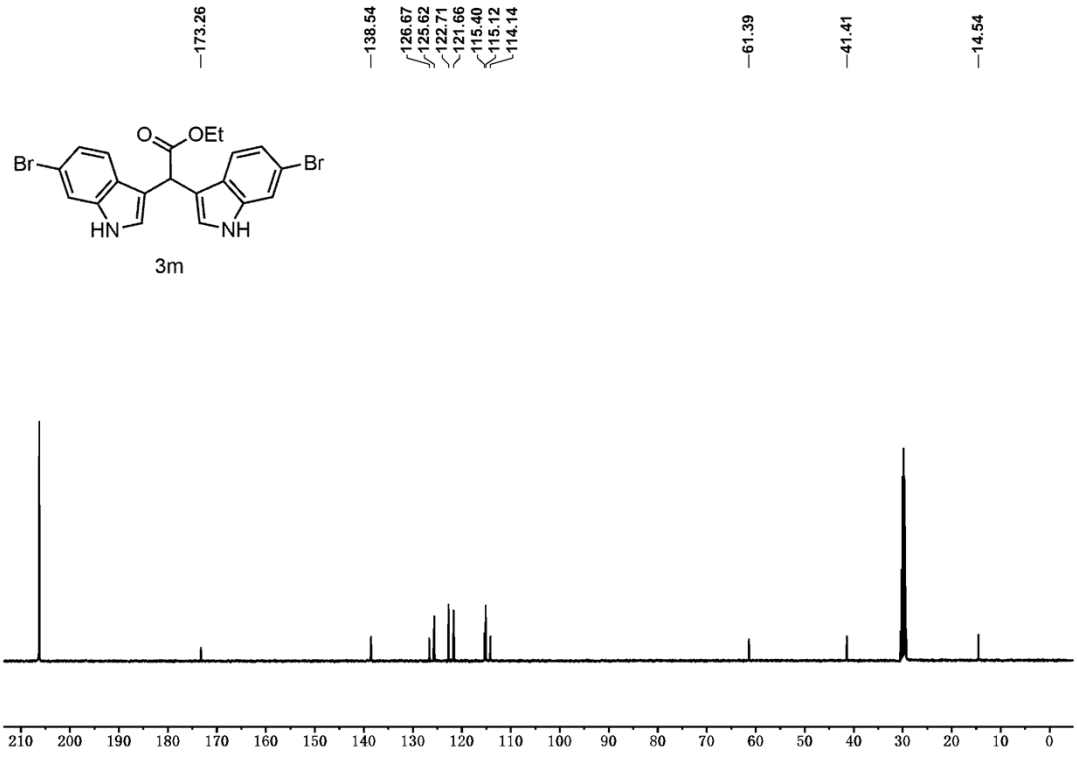
173.26
138.54
126.67
125.62
122.71
121.66
115.40
115.12
114.14
61.39
41.41
14.54
O
OEt
Br
Br
HN
NH
3m
210 200 190 180 170 160 150 140 130 120 110 100 90 80 70 60 50 40 30 20 10 0

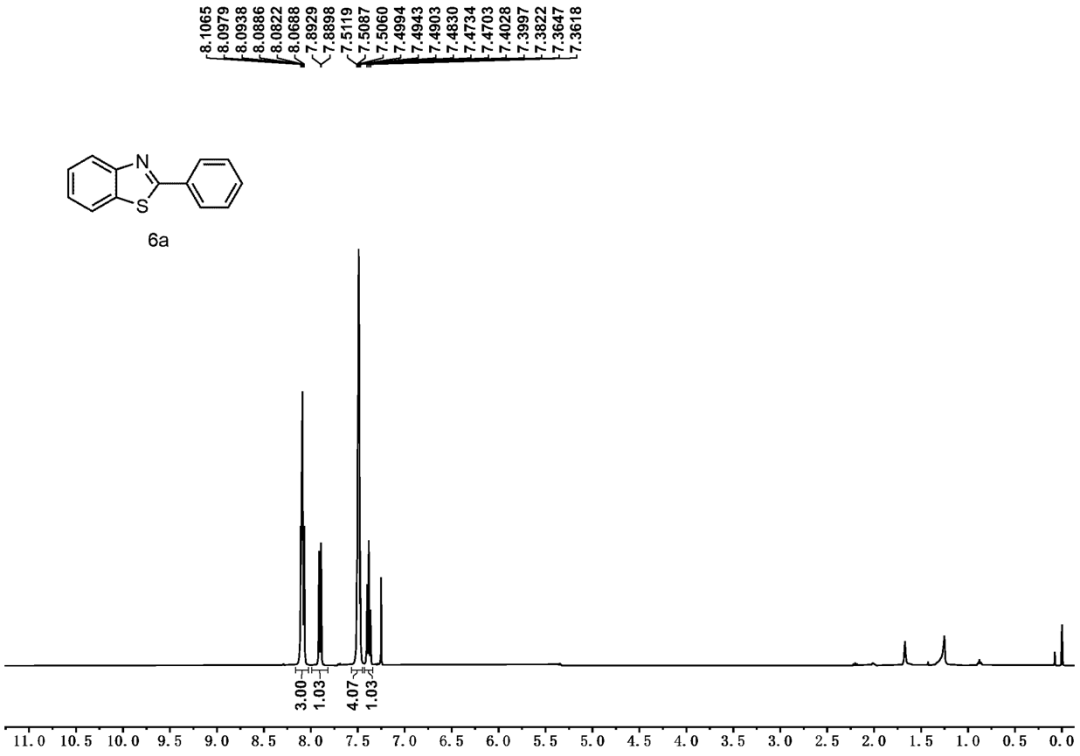
8.1065
8.0979
8.0938
8.0886
8.0822
8.0688
7.8929
7.8898
7.5119
7.5087
7.5060
7.4994
7.4943
7.4903
7.4830
7.4734
7.4703
7.4028
7.3997
7.3822
7.3647
7.3618
N
S
6a
3.00
1.03
4.07
1.03
11.0 10.5 10.0 9.5 9.0 8.5 8.0 7.5 7.0 6.5 6.0 5.5 5.0 4.5 4.0 3.5 3.0 2.5 2.0 1.5 1.0 0.5 0.0

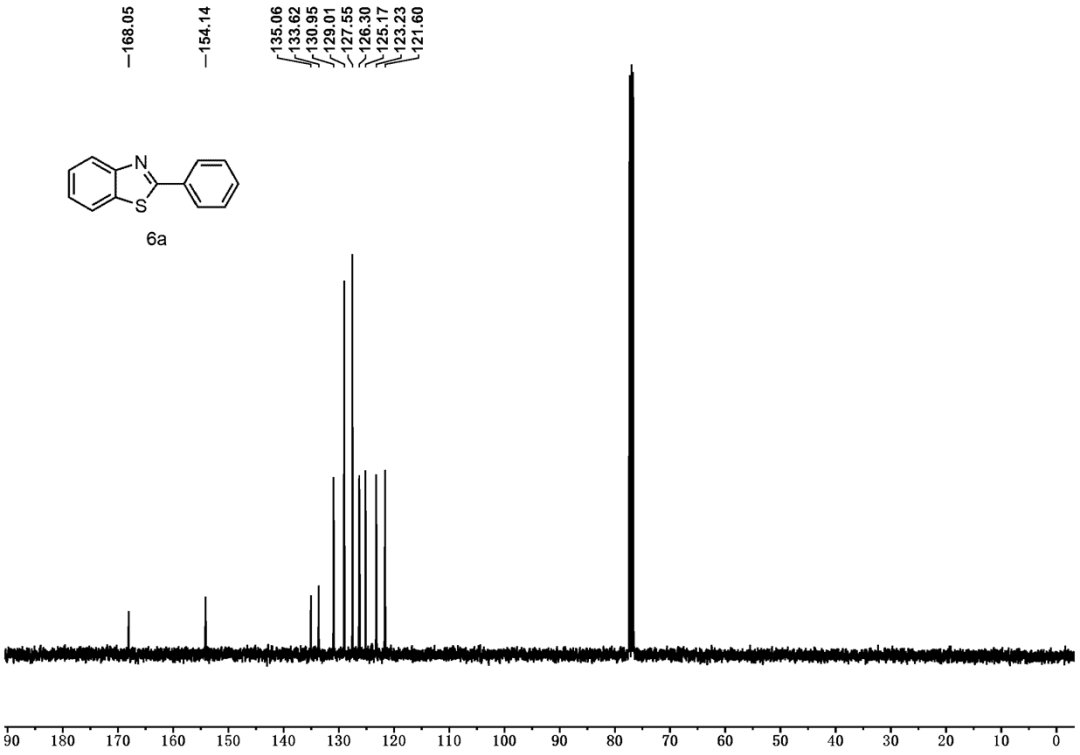
168.05
154.14
135.06
133.62
130.95
129.01
127.55
126.30
125.17
123.23
121.60
N
S
6a
90 180 170 160 150 140 130 120 110 100 90 80 70 60 50 40 30 20 10 0

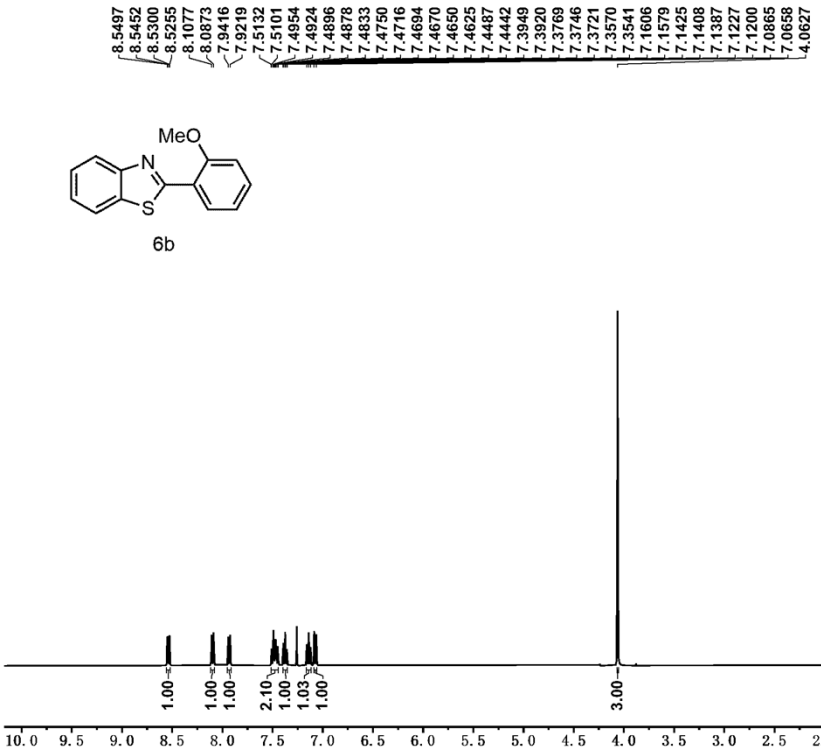
8.5497
8.5452
8.5300
8.5255
8.1077
8.0873
7.9416
7.9219
7.5132
7.5101
7.4954
7.4924
7.4896
7.4878
7.4833
7.4750
7.4716
7.4694
7.4670
7.4650
7.4625
7.4487
7.4442
7.3949
7.3920
7.3769
7.3746
7.3721
7.3570
7.3541
7.1606
7.1579
7.1425
7.1408
7.1387
7.1227
7.1200
7.0865
7.0658
4.0627
MeO
N
S
6b
1.00
1.00
1.00
2.10
1.00
1.03
1.00
3.00
10.0
9.5
9.0
8.5
8.0
7.5
7.0
6.5
6.0
5.5
5.0
4.5
4.0
3.5
3.0
2.5
2.0
1.5
1.0
0.5
0.0

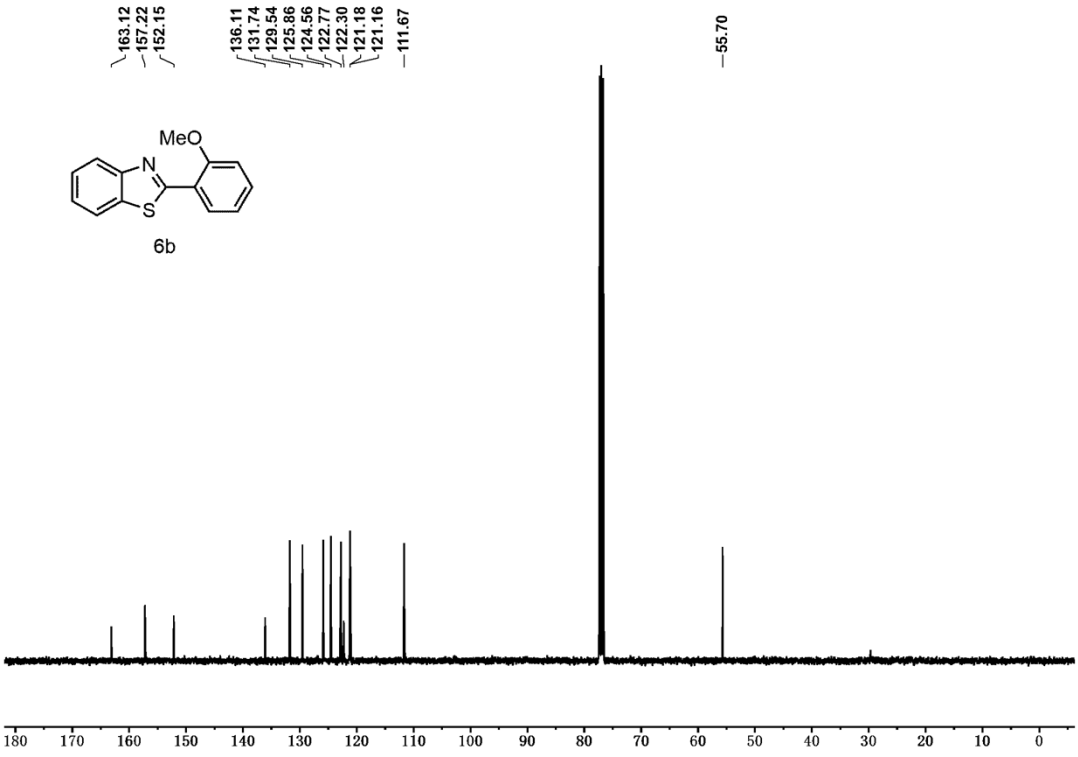
163.12
157.22
152.15
136.11
131.74
129.54
125.86
124.56
122.77
122.30
121.18
121.16
111.67
55.70
MeO
N
S
6b
180
170
160
150
140
130
120
110
100
90
80
70
60
50
40
30
20
10
0

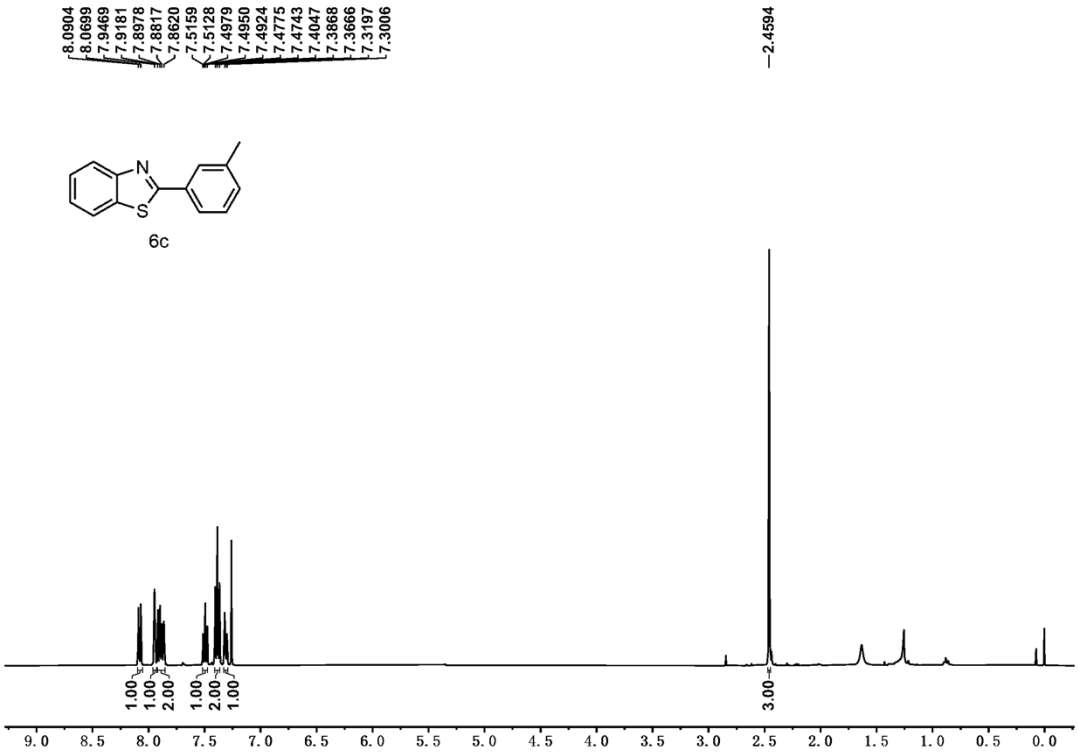
8.0904
8.0699
7.9469
7.9181
7.8978
7.8817
7.8620
7.5159
7.5128
7.4979
7.4950
7.4924
7.4775
7.4743
7.4047
7.3868
7.3666
7.3197
7.3006
2.4594
N
S
6c
1.00
1.00
2.00
1.00
2.00
1.00
3.00
9.0
8.5
8.0
7.5
7.0
6.5
6.0
5.5
5.0
4.5
4.0
3.5
3.0
2.5
2.0
1.5
1.0
0.5
0.0

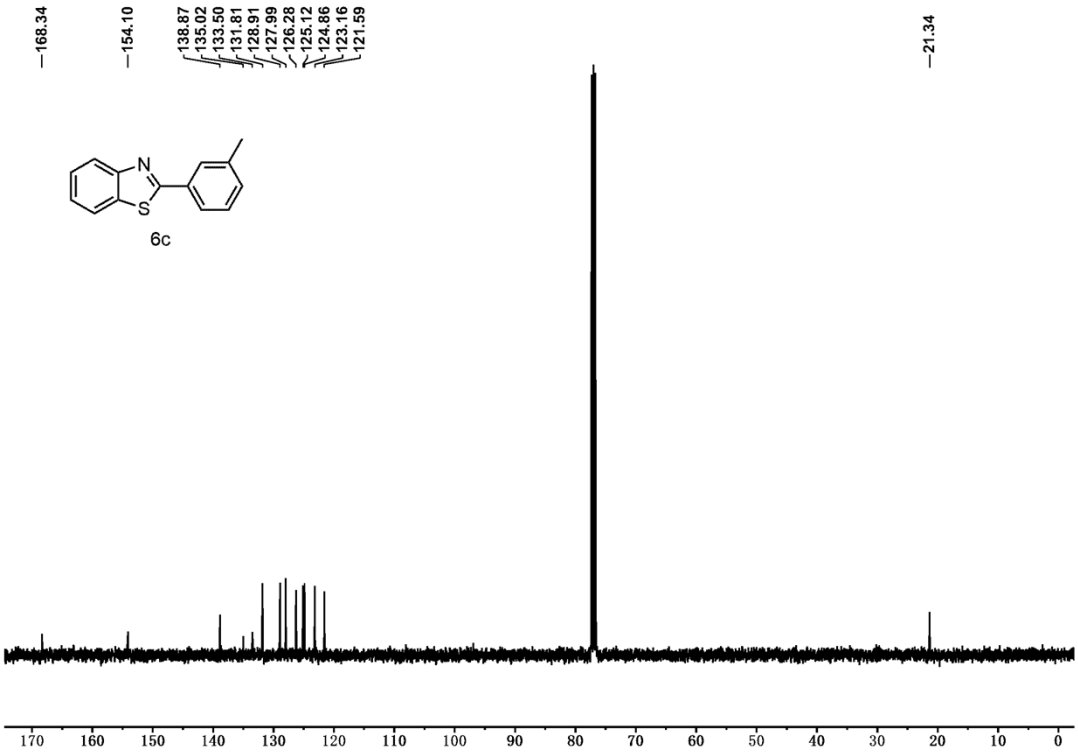
168.34
154.10
138.87
135.02
133.50
131.81
128.91
127.99
126.28
125.12
124.86
123.16
121.59
21.34
N
S
6c
170
160
150
140
130
120
110
100
90
80
70
60
50
40
30
20
10
0


8.0786
8.0583
7.9724
7.9661
7.9612
7.9496
7.9447
7.9383
7.9093
7.8911
7.6404
7.6342
7.6292
7.6175
7.6128
7.6064
7.5239
7.5207
7.5059
7.5029
7.5001
7.4854
7.4822
7.4206
7.4176
7.4027
7.4002
7.3976
7.3826
7.3797

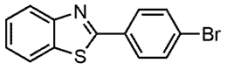
N
S
Br

6d

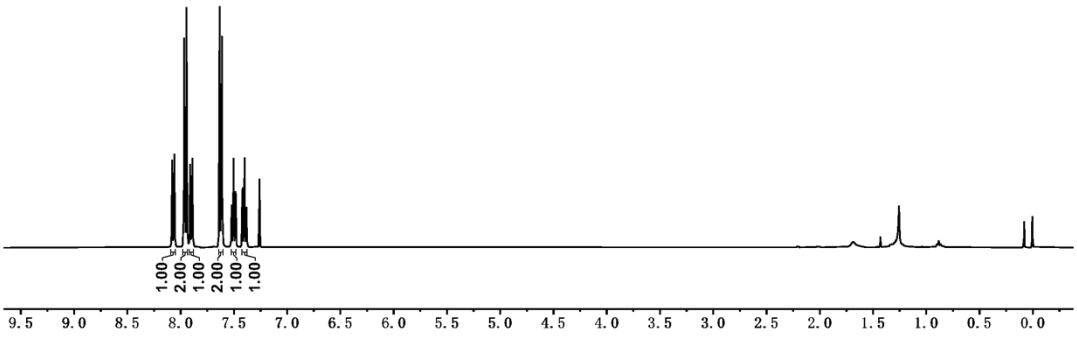
1.00
2.00
1.00
2.00
1.00
1.00
9.5
9.0
8.5
8.0
7.5
7.0
6.5
6.0
5.5
5.0
4.5
4.0
3.5
3.0
2.5
2.0
1.5
1.0
0.5
0.0

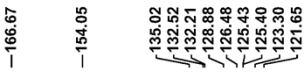
166.67
154.05
135.02
132.52
132.21
128.88
126.48
125.43
125.40
123.30
121.65

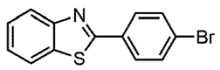
N
S
Br

6d

180
170
160
150
140
130
120
110
100
90
80
70
60
50
40
30
20
10
0

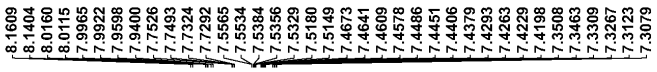
8.1609
8.1404
8.0160
8.0115
7.9965
7.9922
7.9598
7.9400
7.7526
7.7493
7.7324
7.7292
7.5565
7.5534
7.5384
7.5356
7.5329
7.5180
7.5149
7.4673
7.4641
7.4609
7.4578
7.4486
7.4451
7.4406
7.4379
7.4293
7.4263
7.4229
7.4198
7.3508
7.3463
7.3309
7.3267
7.3123
7.3079

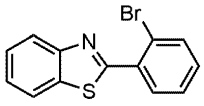
Br
N
S

6e

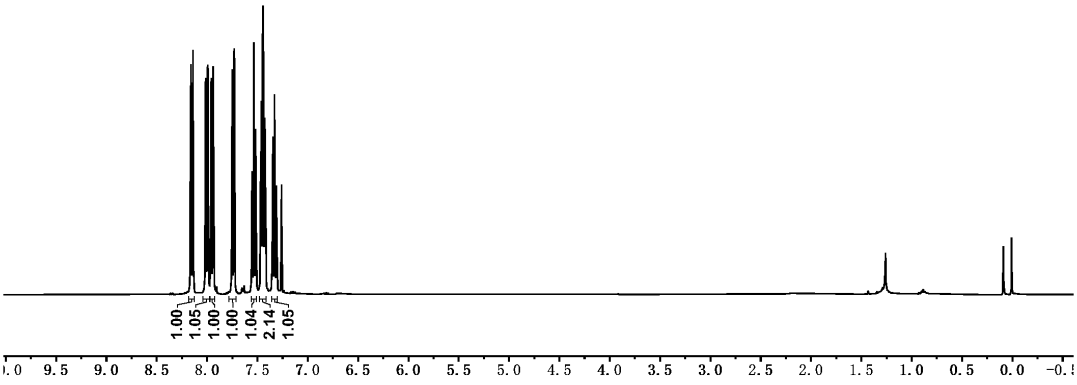
1.00
1.05
1.00
1.00
1.04
2.14
1.05
9.5
9.0
8.5
8.0
7.5
7.0
6.5
6.0
5.5
5.0
4.5
4.0
3.5
3.0
2.5
2.0
1.5
1.0
0.5
0.0

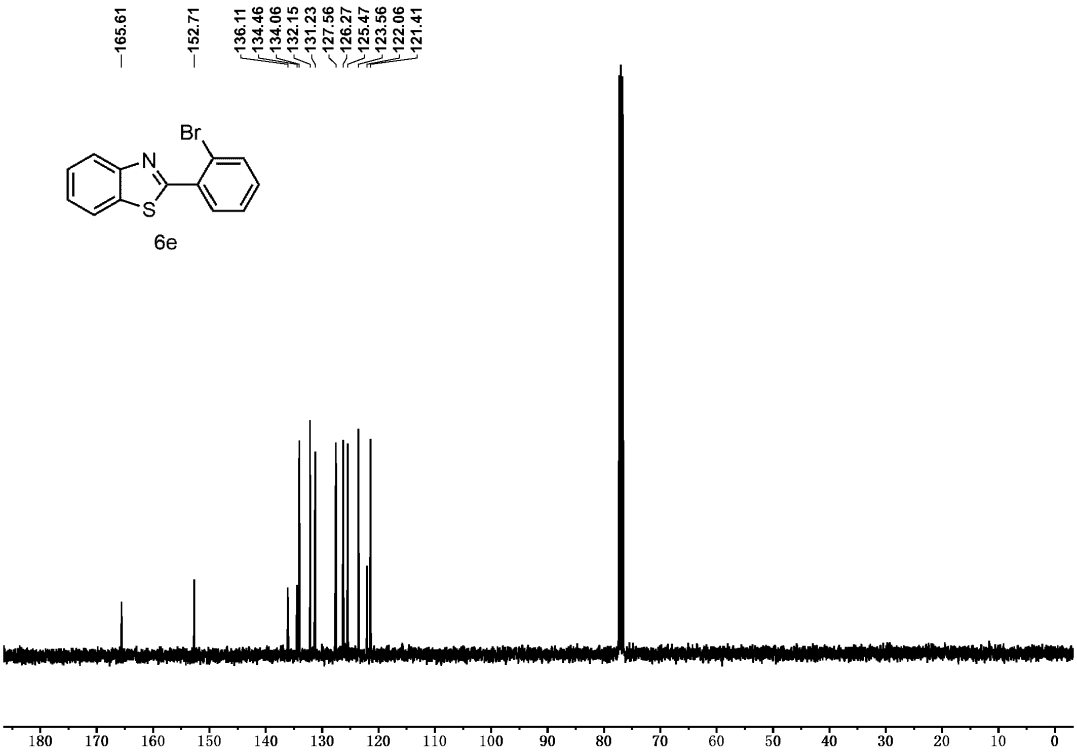
165.61
152.71
136.11
134.46
134.06
132.15
131.23
127.56
126.27
125.47
123.56
122.06
121.41
Br
N
S
180
170
160
150
140
130
120
110
100
90
80
70
60
50
40
30
20
10
0

6e

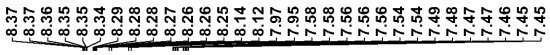
8.37
8.37
8.36
8.35
8.35
8.34
8.29
8.28
8.28
8.27
8.26
8.26
8.25
8.14
8.12
7.97
7.95
7.58
7.58
7.56
7.56
7.56
7.54
7.54
7.49
7.48
7.47
7.47
7.46
7.45
7.45

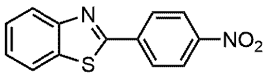
N
S
NO2

6f

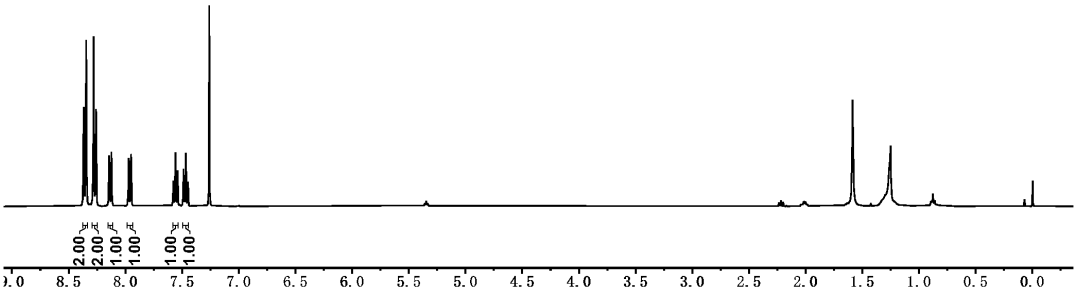
2.00
2.00
1.00
1.00
1.00
1.00
9.0
8.5
8.0
7.5
7.0
6.5
6.0
5.5
5.0
4.5
4.0
3.5
3.0
2.5
2.0
1.5
1.0
0.5
0.0

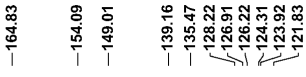
164.83
154.09
149.01
139.16
135.47
128.22
126.91
126.22
124.31
123.92
121.83

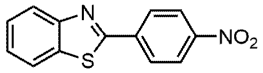
N
S
NO2

6f

170
160
150
140
130
120
110
100
90
80
70
60
50
40
30
20
10
0

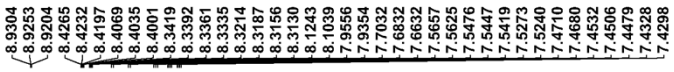
8.9304
8.9253
8.9204
8.4265
8.4232
8.4197
8.4069
8.4035
8.4001
8.3419
8.3392
8.3361
8.3335
8.3214
8.3187
8.3156
8.3130
8.1243
8.1039
7.9556
7.9354
7.7032
7.6832
7.6632
7.5657
7.5625
7.5476
7.5447
7.5419
7.5273
7.5240
7.4710
7.4680
7.4532
7.4506
7.4479
7.4328
7.4298

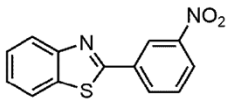
NO2
N
S

6g

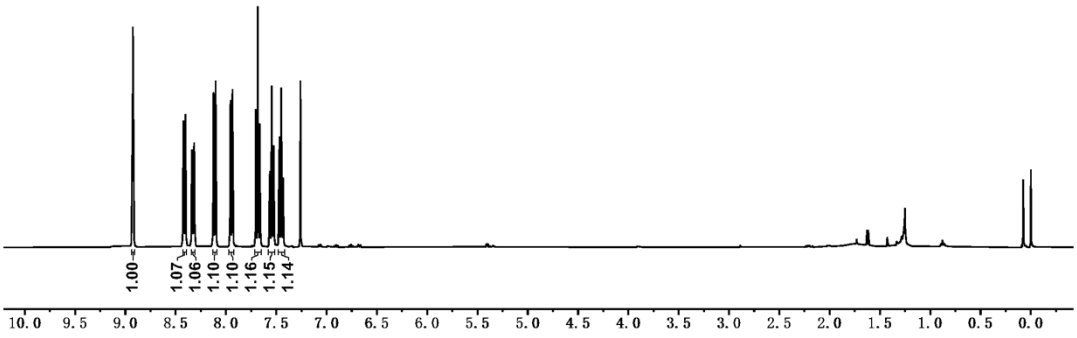
1.00
1.07
1.06
1.10
1.10
1.16
1.15
1.14
10.0
9.5
9.0
8.5
8.0
7.5
7.0
6.5
6.0
5.5
5.0
4.5
4.0
3.5
3.0
2.5
2.0
1.5
1.0
0.5
0.0

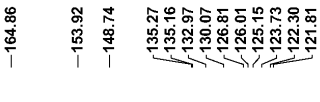
164.86
153.92
148.74
135.27
135.16
132.97
130.07
126.81
126.01
125.15
123.73
122.30
121.81

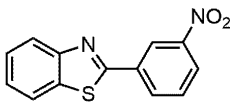
NO2
N
S

6g

170
160
150
140
130
120
110
100
90
80
70
60
50
40
30
20
10
0

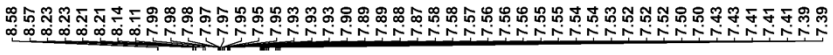
8.58
8.57
8.23
8.23
8.21
8.21
8.14
8.11
7.99
7.98
7.98
7.97
7.97
7.95
7.95
7.95
7.93
7.93
7.93
7.90
7.89
7.89
7.88
7.87
7.58
7.58
7.57
7.56
7.56
7.56
7.55
7.55
7.54
7.54
7.53
7.52
7.52
7.52
7.50
7.50
7.43
7.41
7.41
7.41
7.39
7.39

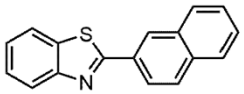
S
N

6h

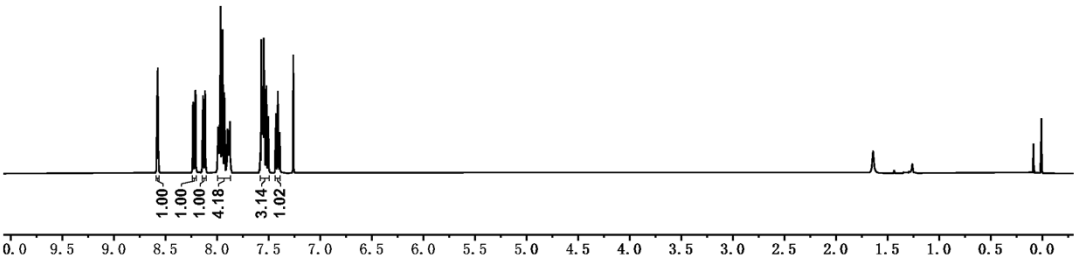
1.00
1.00
1.00
4.18
3.14
1.02
0.0
9.5
9.0
8.5
8.0
7.5
7.0
6.5
6.0
5.5
5.0
4.5
4.0
3.5
3.0
2.5
2.0
1.5
1.0
0.5
0.0

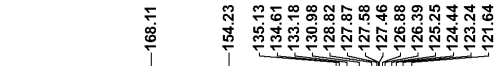
168.11
154.23
135.13
134.61
133.18
130.98
128.82
127.87
127.58
127.46
126.88
126.39
125.25
124.44
123.24
121.64

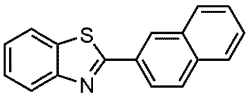
S
N

6h

190
180
170
160
150
140
130
120
110
100
90
80
70
60
50
40
30
20
10


8.0460
8.0253
7.8430
7.8235
7.6490
7.6460
7.6396
7.6367
7.4987
7.4958
7.4895
7.4862
7.4831
7.4715
7.4685
7.4657
7.4510
7.4478
7.3762
7.3732
7.3581
7.3559
7.3533
7.3381
7.3352
7.1315
7.1222
7.1189
7.1096

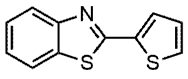

6i

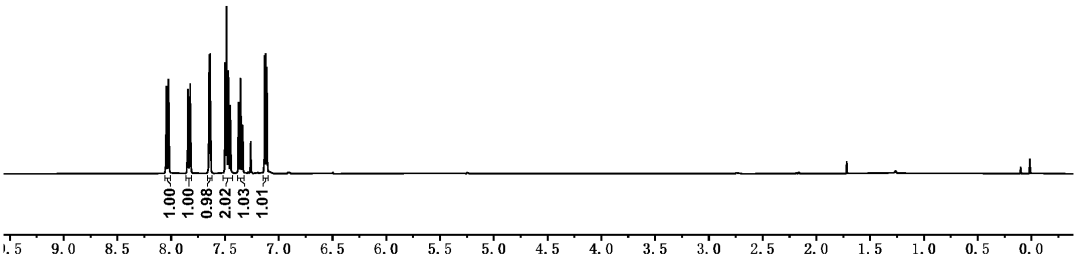
1.00
1.00
0.98
2.02
1.03
1.01
9.0
8.5
8.0
7.5
7.0
6.5
6.0
5.5
5.0
4.5
4.0
3.5
3.0
2.5
2.0
1.5
1.0
0.5
0.0

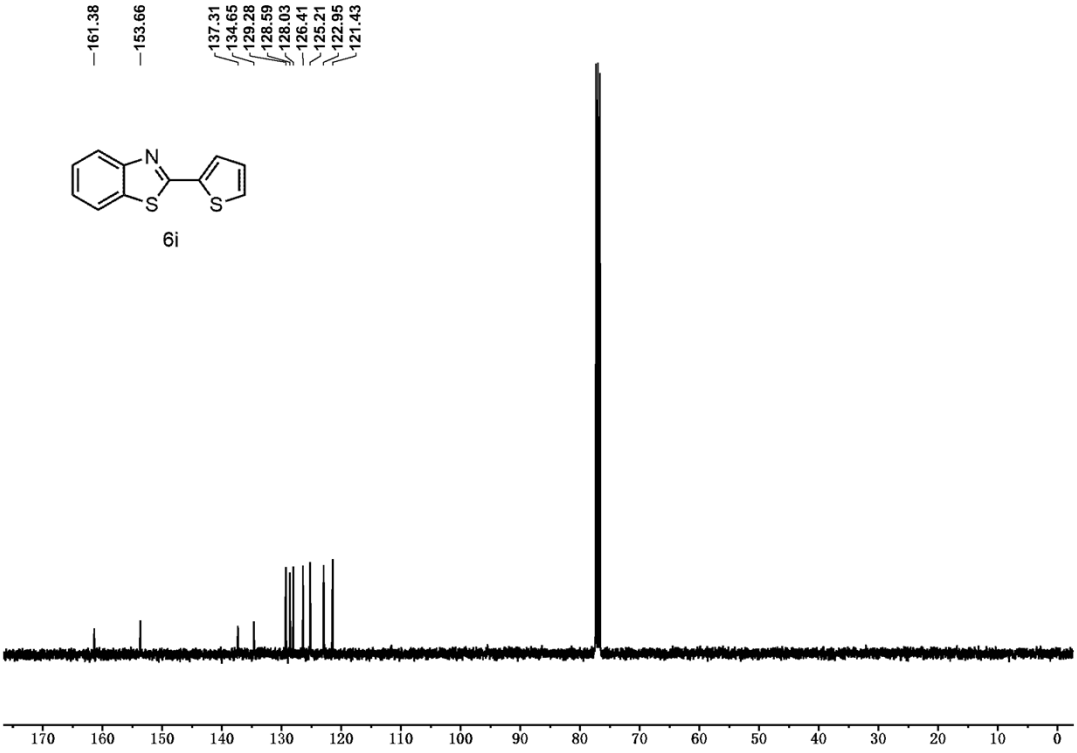
161.38
153.66
137.31
134.65
129.28
128.59
128.03
126.41
125.21
122.95
121.43
170
160
150
140
130
120
110
100
90
80
70
60
50
40
30
20
10
0

6i


8.0492
8.0286
7.8517
7.8317
7.5645
7.5602
7.4604
7.4573
7.4545
7.4399
7.4367
7.3565
7.3535
7.3384
7.3360
7.3334
7.1699
7.1612
6.5578
6.5534
6.5492
6.5446

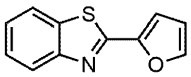
S
N
O

6j

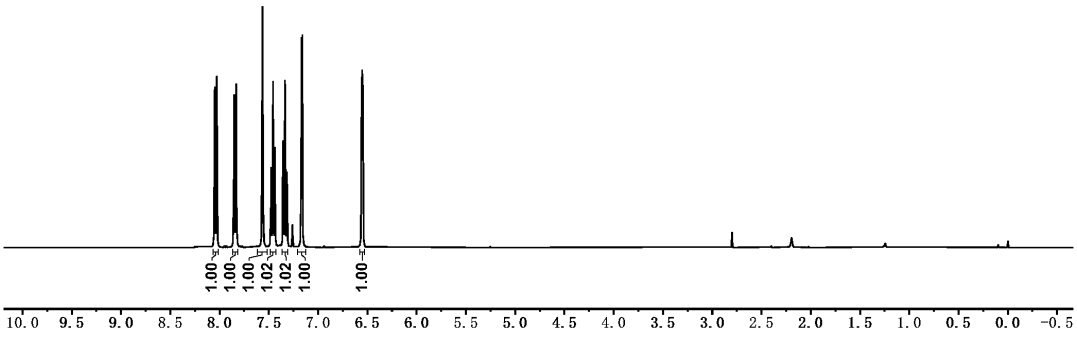
1.00
1.00
1.00
1.02
1.02
1.00
1.00
10.0 9.5 9.0 8.5 8.0 7.5 7.0 6.5 6.0 5.5 5.0 4.5 4.0 3.5 3.0 2.5 2.0 1.5 1.0 0.5 0.0 -0.5

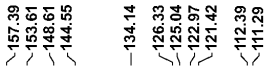
157.39
153.61
148.61
144.55
134.14
126.33
125.04
122.97
121.42
112.39
111.29

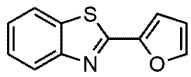
S
N
O

6j

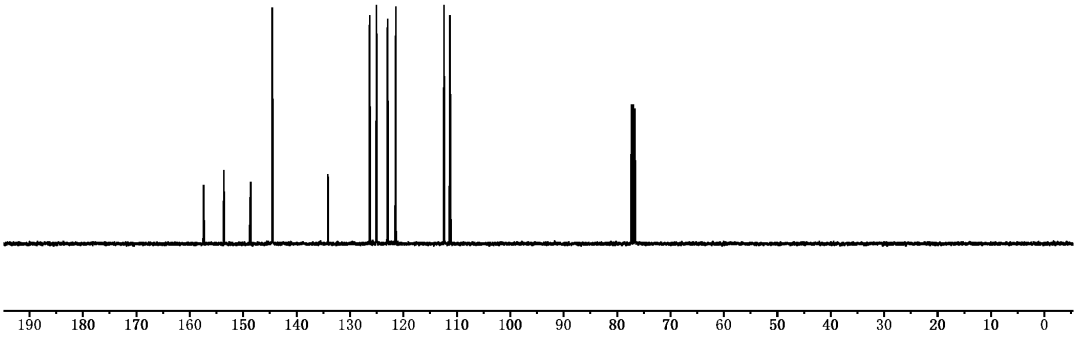
190 180 170 160 150 140 130 120 110 100 90 80 70 60 50 40 30 20 10 0

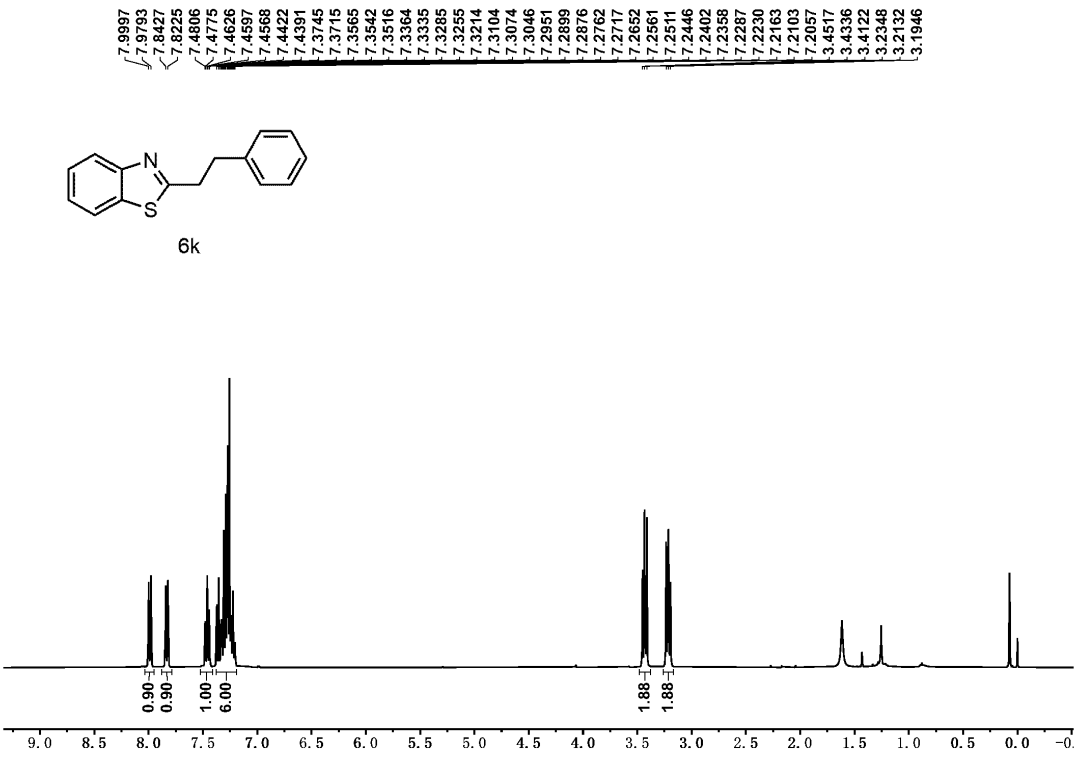
7.9997
7.9793
7.8427
7.8225
7.4806
7.4775
7.4626
7.4597
7.4568
7.4422
7.4391
7.3745
7.3715
7.3565
7.3542
7.3516
7.3364
7.3335
7.3285
7.3255
7.3214
7.3104
7.3074
7.3046
7.2951
7.2899
7.2876
7.2762
7.2717
7.2652
7.2561
7.2511
7.2446
7.2402
7.2358
7.2287
7.2230
7.2163
7.2103
7.2057
3.4517
3.4336
3.4122
3.2348
3.2132
3.1946
N
S
6k
0.90
0.90
1.00
6.00
1.88
1.88
9.0
8.5
8.0
7.5
7.0
6.5
6.0
5.5
5.0
4.5
4.0
3.5
3.0
2.5
2.0
1.5
1.0
0.5
0.0

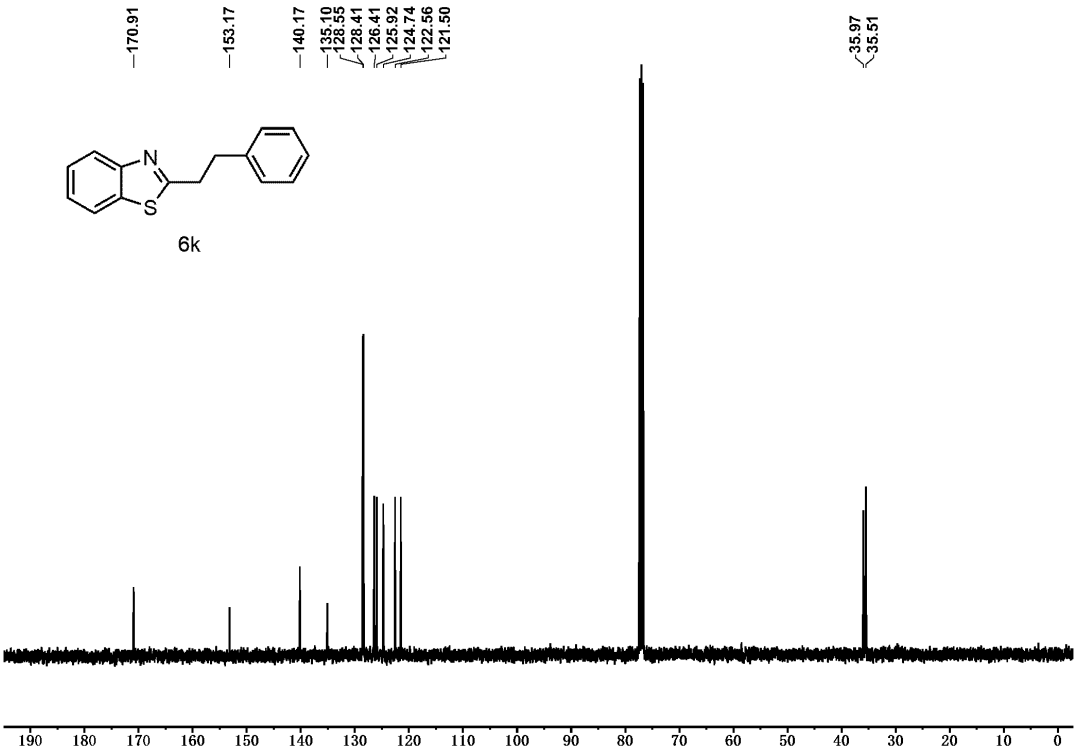
170.91
153.17
140.17
135.10
128.55
128.41
126.41
125.92
124.74
122.56
121.50
35.97
35.51
N
S
6k
190
180
170
160
150
140
130
120
110
100
90
80
70
60
50
40
30
20
10
0

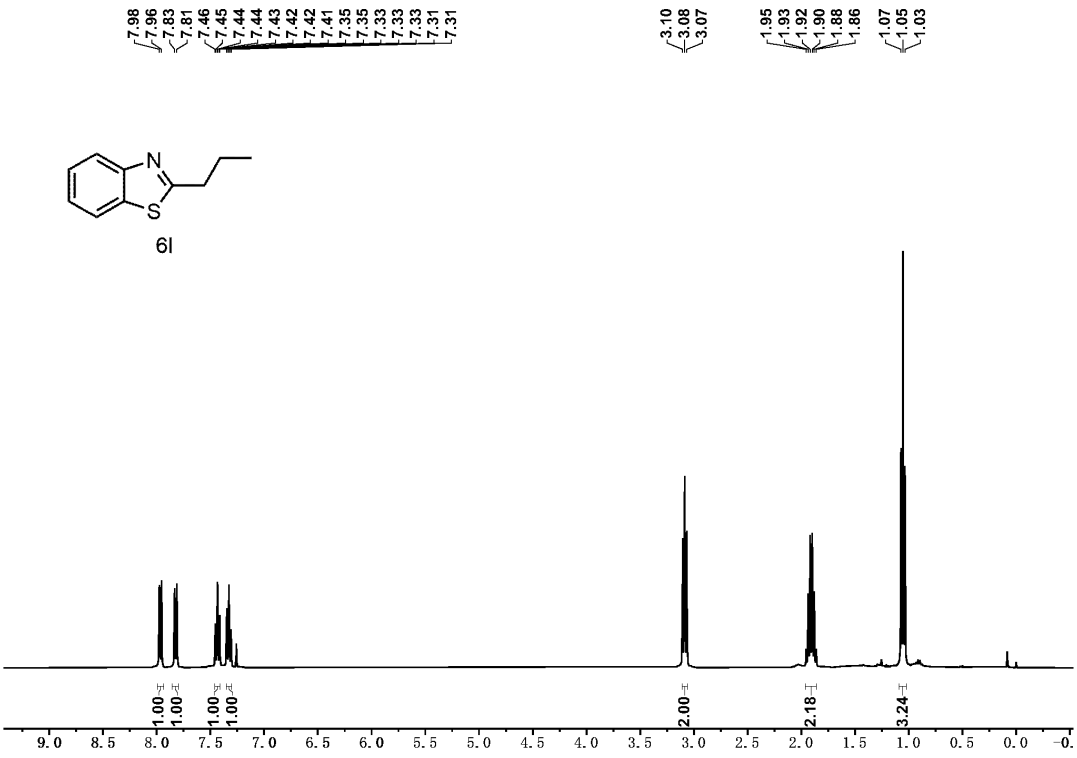
7.98
7.96
7.83
7.81
7.46
7.45
7.44
7.44
7.43
7.42
7.42
7.41
7.35
7.33
7.33
7.31
7.31
3.10
3.08
3.07
1.95
1.93
1.92
1.90
1.88
1.86
1.07
1.05
1.03
6l
1.00
1.00
1.00
1.00
2.00
2.18
3.24

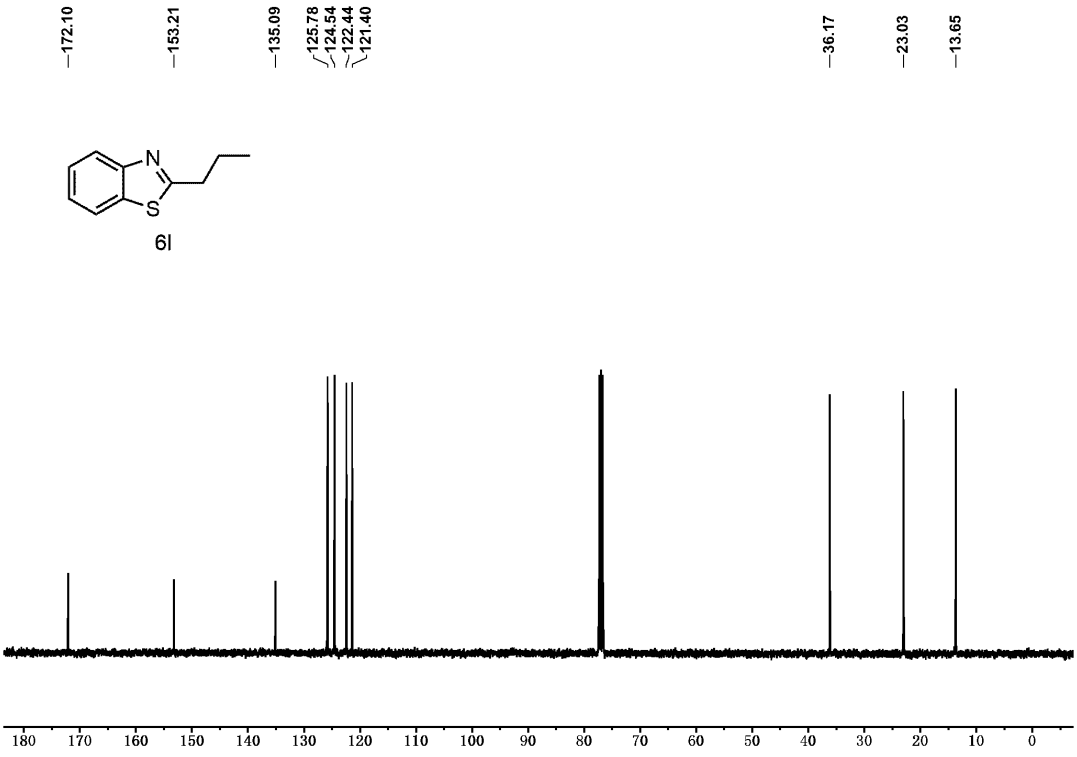
172.10
153.21
135.09
125.78
124.54
122.44
121.40
36.17
23.03
13.65
6l